



Calhoun: The NPS Institutional Archive

Theses and Dissertations

Thesis Collection

1966

Shallow water hydroacoustic communications.

Radecki, Richard Anthony.

Massachusetts Institute of Technology

<http://hdl.handle.net/10945/9633>



Calhoun is a project of the Dudley Knox Library at NPS, furthering the precepts and goals of open government and government transparency. All information contained herein has been approved for release by the NPS Public Affairs Officer.

**Dudley Knox Library / Naval Postgraduate School
411 Dyer Road / 1 University Circle
Monterey, California USA 93943**

<http://www.nps.edu/library>

NPS ARCHIVE
1966
RADECKI, R.

SHALLOW WATER HYDROACOUSTIC COMMUNICATIONS

by

RICHARD ANTHONY RADECKI

MASSACHUSETTS INSTITUTE OF TECHNOLOGY

Thesis
R135

MAY, 1966

**DUDLEY KNOX LIBRARY
NAVAL POSTGRADUATE SCHOOL
MONTEREY, CA 93943-5101**

Library
Naval Postgraduate School
Monterey, California

SHALLOW WATER HYDROACOUSTIC COMMUNICATIONS

by

Richard Anthony Radecki

B.S., United States Naval Academy
1959

SUBMITTED IN PARTIAL FULFILLMENT OF THE REQUIREMENTS
FOR THE DEGREES OF NAVAL ENGINEER AND MASTER
OF SCIENCE (ELECTRICAL ENGINEERING)

at the

MASSACHUSETTS INSTITUTE OF TECHNOLOGY

June, 1966

Signature of Author
Department of Naval Architecture and Marine Engineering,
May 20, 1966

Certified by
Thesis Supervisor

Accepted by
Chairman, Departmental Committee on Graduate Students

City
S. Alvin Postgraduate School
San Mateo, California

~~1965~~
~~1965~~

NPS ARCHIVE

1966

RADECKI, R.

SHALLOW WATER HYDROACOUSTIC COMMUNICATIONS

by

RICHARD ANTHONY RADECKI

Submitted to the Department of Naval Architecture and Marine Engineering on May 20, 1966 in partial fulfillment of the requirements for the Master of Science degree in Electrical Engineering and the Professional degree, Naval Engineer.

ABSTRACT

Hydroacoustic communication has not been used extensively at ranges in excess of ten miles. A study of the shallow-water and surface ducting channels indicate that reliable sixty word per minute communication at ranges of fifty miles is possible under a variety of conditions, with reasonable power levels and equipment complexity. The channel can be approximated by a Rayleigh fading signal with additive Gaussian noise. Five frequency multiplexed binary channels are compared with a fifteen channel system utilizing frequency diversity, and with a fifteen channel system utilizing coding. A method of calculating the diversity error for components with unequal signal and or noise levels is worked out. Frequencies must be above 900 cps if shipping noise is significant, and below 1500 cps to minimize attenuation. To optimize several transmitter-receiver parameters, such as the signal interval, more long range experimental data is required.

Thesis Supervisor: Robert G. Gallager
Title: Associate Professor of Electrical Engineering

ACKNOWLEDGEMENTS

I would like to thank Professor Robert G. Gallagher for his time, patience, and inspiring comments without which this thesis would not have been possible.

I would also like to thank Professor Patrick Leehey for his comments on acoustics in the early portions of the work, my wife, Mary Pat, for her constant inspiration, and Mrs. Emy Korkolis for typing the manuscript.

CONTENTS

	page
Title Page	
Abstract	
Acknowledgements	iii
Contents	iv
List of Diagrams and Illustrations	vi
Introduction	1
Part I. The Shallow Water Hydroacoustic Channel	3
1. General	3
2. The Surface Channel	3
3. The Bottom Reflection Channel	8
4. Noise	12
5. Source Power	14
6. Random Process Channel Model	15
Part II. Communications Systems	18
1. Frequency Selection	18
2. Binary Signalling	20
3. Channel Capacity and Coding	23
4. Representative Communication Systems	28
5. Suitability of Coding Techniques	33
Part III. Discussion	37
1. General	37
2. Assumptions	37
3. Ocean Conditions and the Channel Model	40

Part IV. Conclusions and Recommendations	42
1. Conclusions	42
2. Recommendations	42
Appendix A. Transmission Loss Calculations	44
1. Surface Channel	44
2. Bottom Reflection Channel	45
Appendix B. Limiting Source Power Calculations	46
1. Cavitation	46
2. Non-Linearity	46
Appendix C. Time Dispersion Calculation	48
Appendix D. Diversity Error Probability Calculation	51
References Cited	55

LIST OF DIAGRAMS AND ILLUSTRATIONS

Figure	page
1. Surface ducting channel.	4
2. Spherical and cylindrical spreading losses.	4
3. Surface channel ray path calculation geometry.	7
4. The SOFAR channel.	7
5. Shallow water velocity profiles.	10
6. The bottom reflection channel.	10
7. Sound pressure level at 50 miles as a function of frequency.	11
8. Ambient noise in the ocean.	13
9. Expected signal-noise separation in a state 3 sea.	19
10. Binary correlation receiver.	22
11. Binary envelope detector receiver.	22
12. Received signal in the s_o -plane and s_r -plane when message $s_o(t)$ is sent.	24
12A. The binary symmetric channel.	24
13. The effect of adding additional higher frequency channels on capacity and rate.	27
14. Three-fold diversity receiver.	31
15. Binary receiver error probabilities for the Rayleigh fading channel.	32
16. The binary erasure channel.	35
17. Convolutional encoder.	35
18. Typical amplitude distributions.	39
19. Effect of a sloping bottom on communications via the bottom reflection channel in shallow water.	39
20. Model for time dispersion calculation.	49
21. Diversity error with unequal signal-noise ratios.	54

INTRODUCTION

Except for a few very short range or very low rate systems, the communications capability of ocean acoustics has not been exploited. Voice modulation has been used extensively for ranges of a few miles and CW at slightly longer ranges. Single explosive charge signals have been sent over a thousand miles via deep ocean channels. Aside from sonar these few examples cover most of the communications development. With the increasing interest in nuclear submarines, oceanography, and the industrialization of underwater real estate, the usefulness of a reliable system which does not depend on radio or cables is apparent.

In this thesis a single such problem will be considered, that is, communication between two stations in relatively shallow water using transducers near the surface. A range of fifty miles and a data rate of sixty words per minute will be used to evaluate various systems. If such a system were feasible it would provide a good link between ships operating in the same geographic area, or between an oceanographic vessel and its remote data collecting stations, or any number of other purposes.

Part I of this thesis will be a simplified description of the shallow water acoustic channel, which will point out the parameters important to a communications system. These include ambient noise levels, transmission losses, and channel stability. These parameters will be used to arrive at a

random process model of the channel.

In Part II this model will be used to develop a communication system. First a single binary channel will be developed. This will then be extended as required to obtain the desired data rate at a range of fifty miles with an acceptable error rate. Since there are many ways to handle the problem only one or two representing current technology will be discussed.

In Part III the feasibility of hydroacoustic communications under various ocean conditions will be evaluated. The assumptions used in the first two parts and their effects will also be evaluated at this point.

Part IV will summarize the results and indicate areas requiring additional research and or development.

Part I

SHALLOW-WATER HYDROACOUSTICS

1. General. In shallow water there are two principle methods of acoustic transmission. The first type is the surface channel. In this channel a large portion of the acoustic energy is trapped in a duct near the surface. Transmission in this duct is by surface reflection and upward refraction. The second type is transmission by both surface and bottom reflections. The particular type of transmission which will occur is primarily dependent on the vertical profile of the velocity of sound in the ocean area. The velocity of sound in sea water varies primarily with temperature and to a lesser degree with pressure and salinity. Over long ranges it is reasonable that both types of transmission may occur for part of the distance.

2. The Surface Channel. The density of water decreases with temperature. This means that in general the water near the surface is warmer. However, if a cooling condition exists, the surface water may be cooler or at the same temperature as deeper water. This inversion causes the surface channel to exist. The velocity of sound increases with increasing pressure and with increasing temperature (1). Therefore, an inversion or isothermal layer will have a positive velocity gradient, i.e., velocity of sound increases with depth. According to Snell's law, acoustic waves in this layer will be bent upward, reflected from the surface and bent upward again. Figure 1 is a diagram of this type of channel. It has been

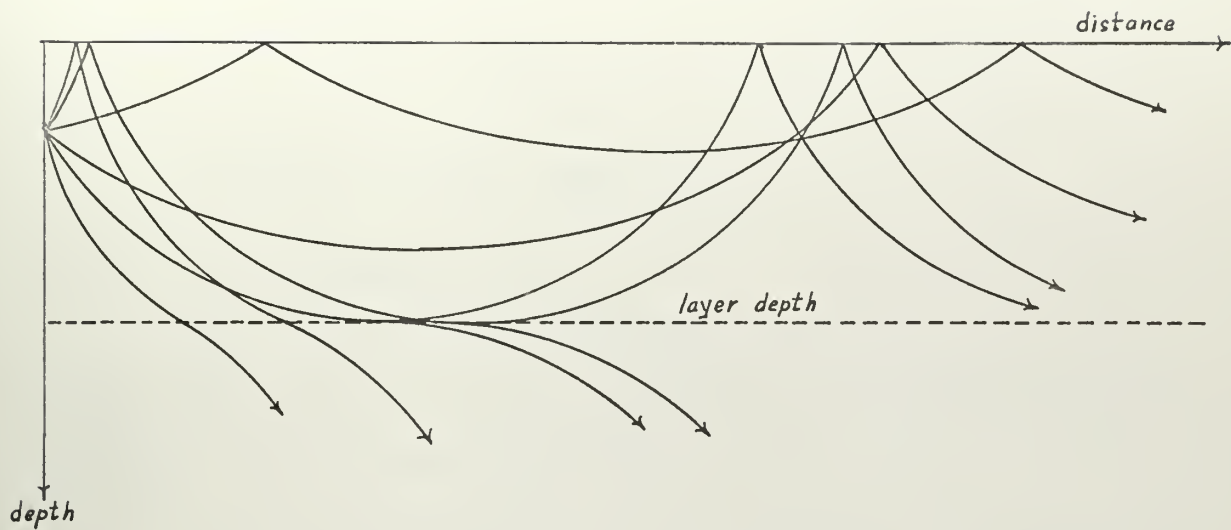


Figure 1. Surface ducting channel.

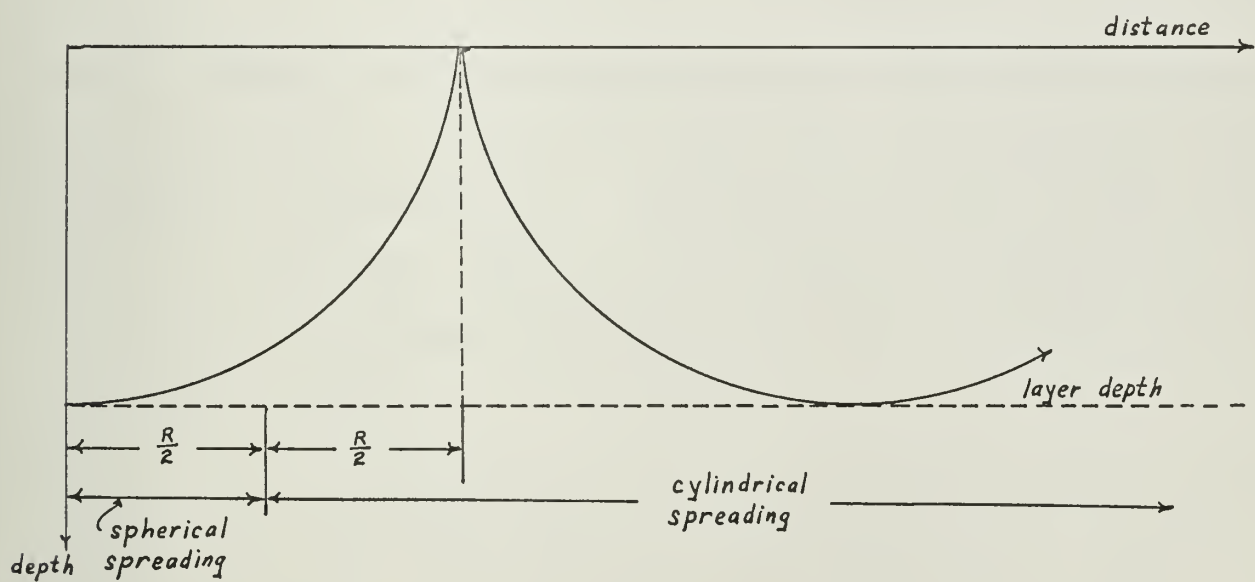


Figure 2. Spherical and cylindrical spreading losses.

shown and experimentally verified, that a minimum layer depth is required to trap a given frequency signal (2). This depth is:

$$L_{\min} = 2.7 \times 10^3 (f_g^2)^{-1/3}$$

f = frequency (cps)

g = duct velocity gradient (sec.⁻¹)

For a 1000 cps signal, and a 0.020 meter/second/meter velocity gradient this minimum layer depth is 304 meters.

There are several types of transmission losses which must be considered in this channel. These are: spreading losses, reflection losses, and absorption losses. The spreading loss will be broken into spherical and cylindrical components. The energy leaves the source initially as a spherical wave. Beyond a certain point the energy is essentially trapped in the layer and the spreading loss becomes cylindrical. For purposes of calculation the transition point will be taken as half the horizontal range of a ray leaving the source at the layer depth horizontally and just reaching the surface. This is shown in figure 2.

The second type of loss to be considered is the surface reflection loss. The reflection coefficient for the water-air interface is approximately minus one. This is true for calm water, but waves cause a certain amount of scatter loss. This loss coefficient has been determined experimentally (3). The following formula describes the loss function for a frequency-waveheight product less than 3:

$$\alpha_1 = -10 \log_{10} (1 - 0.149 (fH)^{3/2}) \text{ db per bounce}$$

f = frequency in kc/sec.

H = waveheight in meters

The third type of loss to be considered is absorption. This takes into account primarily the thermal and viscous forces which are otherwise neglected in deriving the wave equation of acoustics in a liquid medium. For the ranges of interest this loss is negligible below frequencies of 2 kc. A suitable formula for absorption losses which is accurate from frequencies of 2-25 kc is (4) :

$$\alpha_2 = \frac{7200 \times 10^{-6} f^2}{7750 + f^2} + 3.85 \times 10^{-8} f^2 \text{ nepers per meter}$$

this gives a transmission loss of:

$$L = 7.280 \times 10^3 \alpha_2 \text{ db/km.}$$

If it is assumed that the velocity of sound does not vary in the channel except linearly with depth, some rather simple equations can be derived which specify the geometry of the path in depth and range. Referring to figure 3, these formulas are (5):

d = transducer depth (meters)

L = layer depth (meters)

R = horizontal range (meters)

a = velocity gradient (sec.⁻¹)

$\theta = 90^\circ$ - angle of incidence

Y = vertical depth used for calculation (meters)

c_0 = lowest velocity of sound in the layer (meters/sec.)

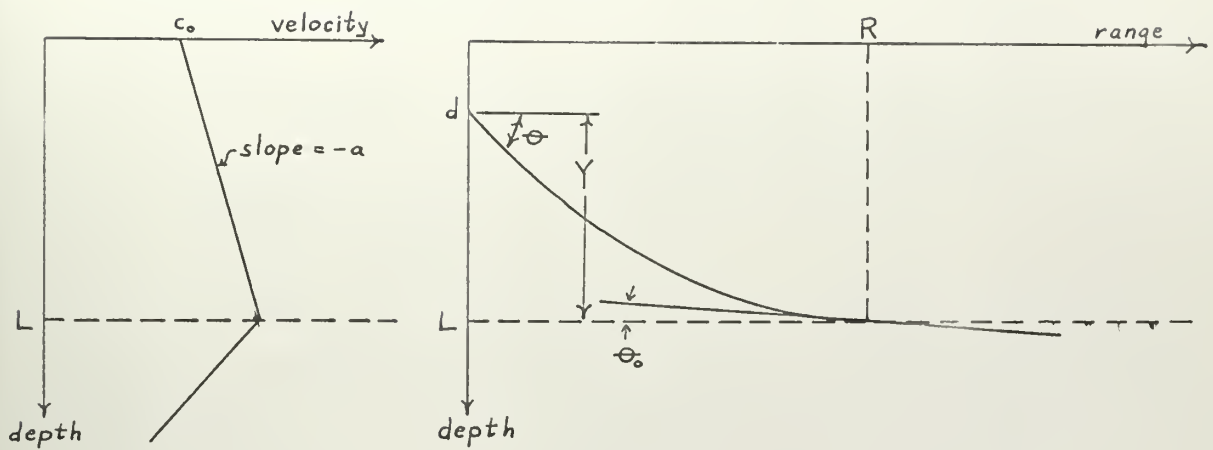
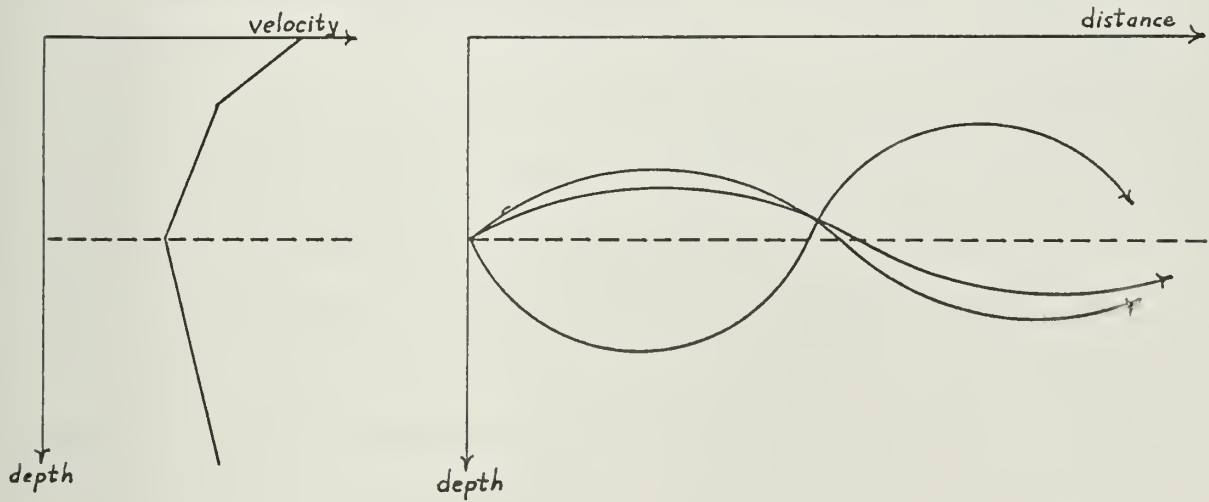


Figure 3. Surface channel ray path calculation geometry.



Velocity profile.

Typical transmission paths.

Figure 4. The SOFAR channel.

$$Y = \frac{c_0}{a \cos \theta_0} (\cos \theta - \cos \theta_0)$$

$$R = \frac{c_0}{a \cos \theta_0} (\sin \theta_0 - \sin \theta)$$

$$\frac{\cos \theta_0}{c_0} = \frac{1}{c_0 + aY}$$

If we now let $Y = L$ (transducer at the surface), and $\theta_0 = 0$ then $2R$ is the maximum distance between reflections, and the minimum number of reflections over a distance D is:

$$\text{minimum number of reflections} = \frac{D}{2R}$$

Since the water depth does not enter any calculations for the surface channel, it is also a suitable deep water model as long as it is uninterrupted.

3. The Bottom Reflection Channel. The bottom reflection channel only exists in shallow water. In very deep water the temperature reaches a minimum at some intermediate depth and is isothermal down to the bottom. This gives rise to a minimum velocity of sound, which generally occurs at depths of about two thousand feet. Sound waves are reflected upward below this depth, and downward above this depth. This is the SOFAR channel shown in figure 4. It will not be considered in this thesis. For the shallow water channel, ocean depths up to 600 meters will be considered. This includes about ten per cent of the oceans, mostly along the continental shelf (6).

In shallow water the SOFAR channel rarely exists, and the effects of both bottom and surface reflections are significant. Some typical linearized velocity profiles are shown

in figure 5. For uniform velocity gradients the ray path equations as described for ^{the} surface channel may be used for the bottom reflection channel path calculations. For a, b, and c of figure 5, these calculations would have to be made in several steps.

Except for the addition of a bottom reflection loss the bottom reflection channel losses are the same as those of the surface channel. Because of the greater channel depth it is obvious that the spherical spreading loss will extend for a greater distance. This will be computed as R vice $R/2$ as ^{for} the surface channel. In general, experimental data shows that the total losses for this type of channel approximate spherical losses for the whole transmission distance. The surface channel has total losses somewhat lower than spherical spreading. The bottom reflection loss is a complex function of the bottom material and its structure. For grazing angles less than fifteen degrees however, the losses are small. A good experimental figure is 0.3 db per bounce (7). For larger grazing angles the loss becomes quite large. Figure 6 is a transmission path diagram of the bottom reflection channel. Note that rays which graze the bottom at about 15 degrees, leave the source at a much smaller angle.

Sample calculations are made for both the surface channel and the bottom reflection channel in Appendix A. Several computations are plotted in figure 7 together with some experimental data for comparison. In all cases the

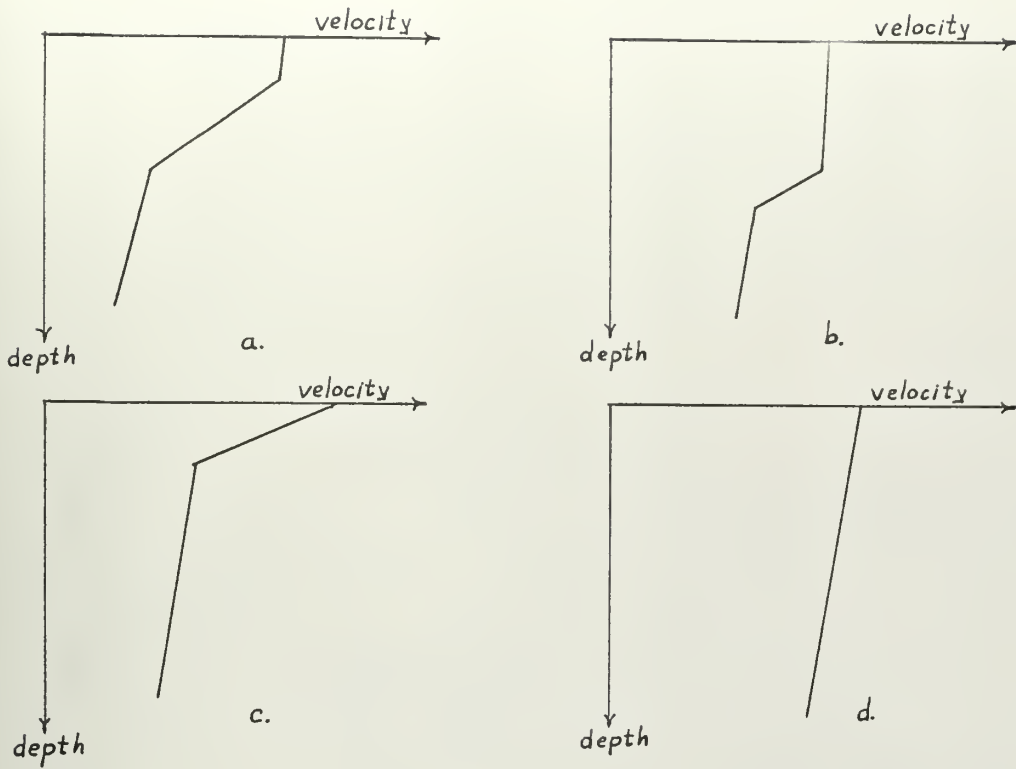


Figure 5. Shallow water velocity profiles.

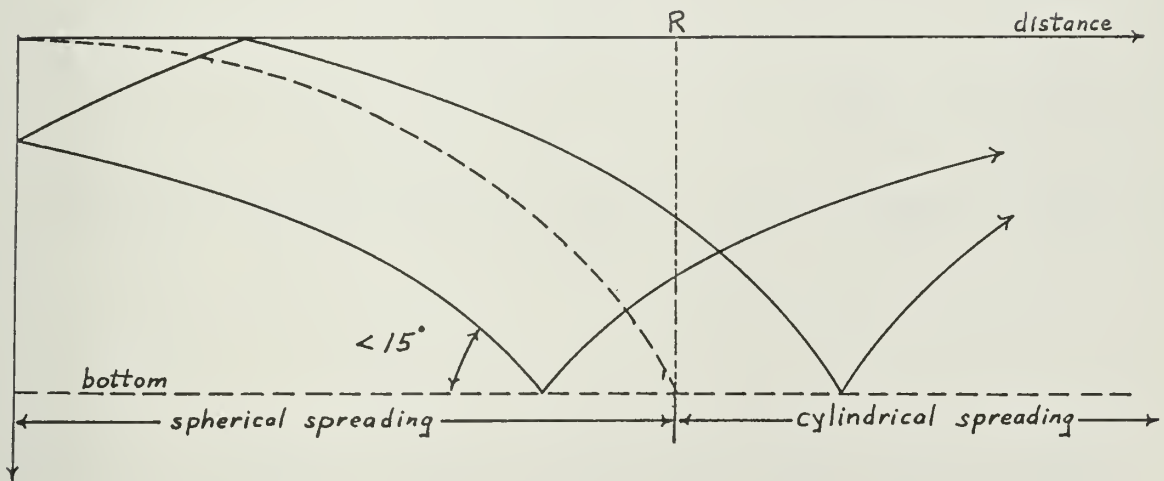


Figure 6. The bottom reflection channel.

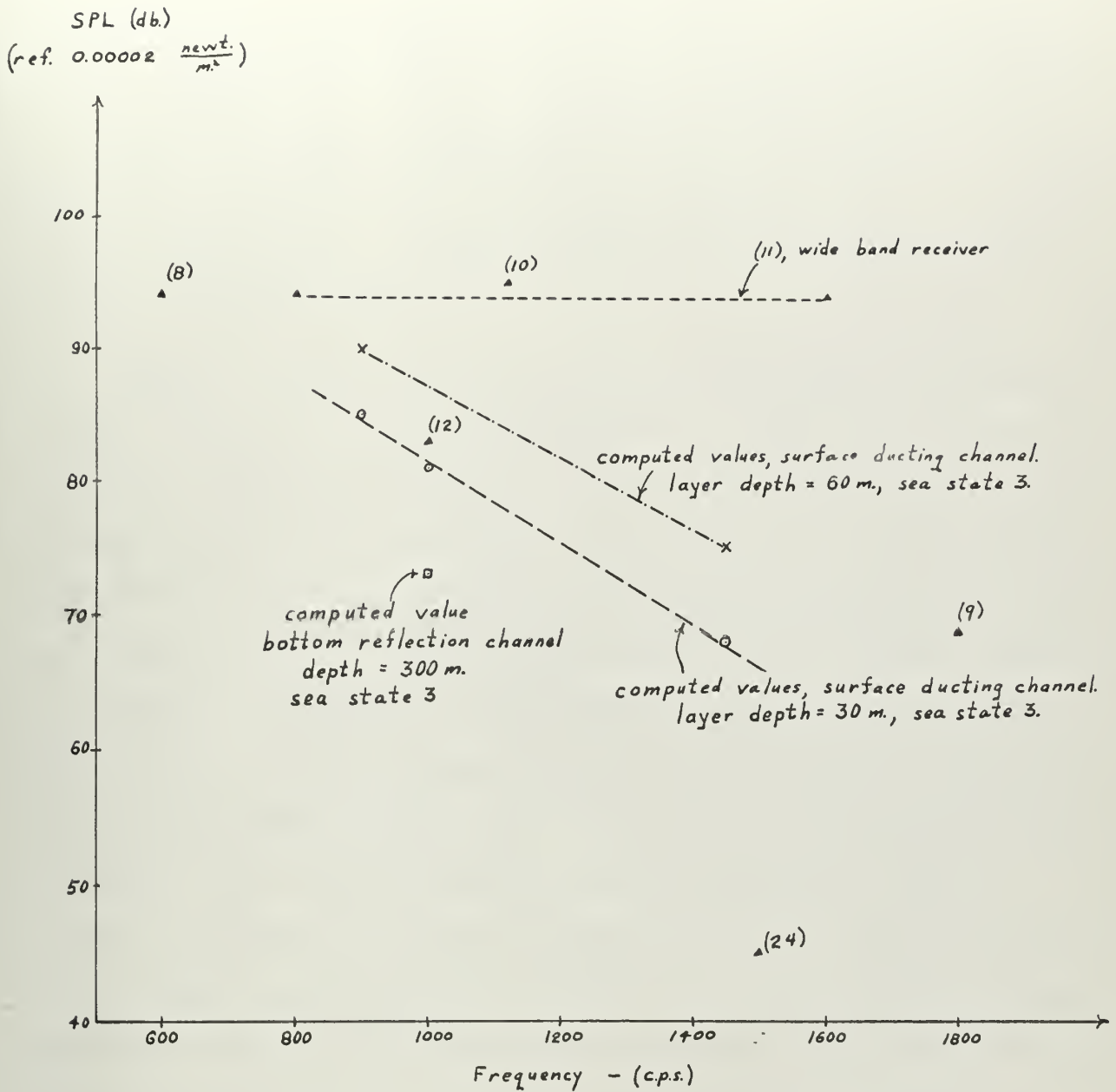


Figure 7. Sound pressure level at 50 miles as a function of frequency. All data corrected to a source level of 179 db. at a radius of one meter. References for experimental data in parentheses.

sources were corrected to a sound pressure level of 185 db (ref. 0.00002 newt./m²) at a 1/4 meter radius.

$$\text{SPL} = 20 \log_{10} \frac{P}{P_0}$$

This is low enough to permit simultaneous transmission over each of ten channels.

4. Noise. Ambient sea noise is a complex array of processes which are not all fully understood (13). Most noise sources are very frequency dependent. Below 1000 cps ship and traffic noise is the most significant. It usually peaks between 300 and 800 cps and falls off rapidly at higher frequencies. For all frequencies of interest above 1000 cps the ambient noise is primarily dependent on sea state for all but calm weather. The primary sources of this noise are thought to be wind, spray, cavitation, and precipitation. Other sources are marine life, molecular and thermal agitation and earthquakes. Table 1 gives the average relations between wind force, wind velocity, wave height, and sea state. Figure 8 is a plot of the average ambient noise in the ocean versus sea state. The highest expected values are about 3 db above the average. A possible explanation is an irregular gusting wind. It should also be noted that deep water noise levels are generally 5 db lower than shallow water levels.

If a transducer is to be carried on a ship, the ship's self noise is very important (14). At low speeds this will correspond to the ambient noise at sea state 2, but it may contain some high level discrete frequencies. At speeds above

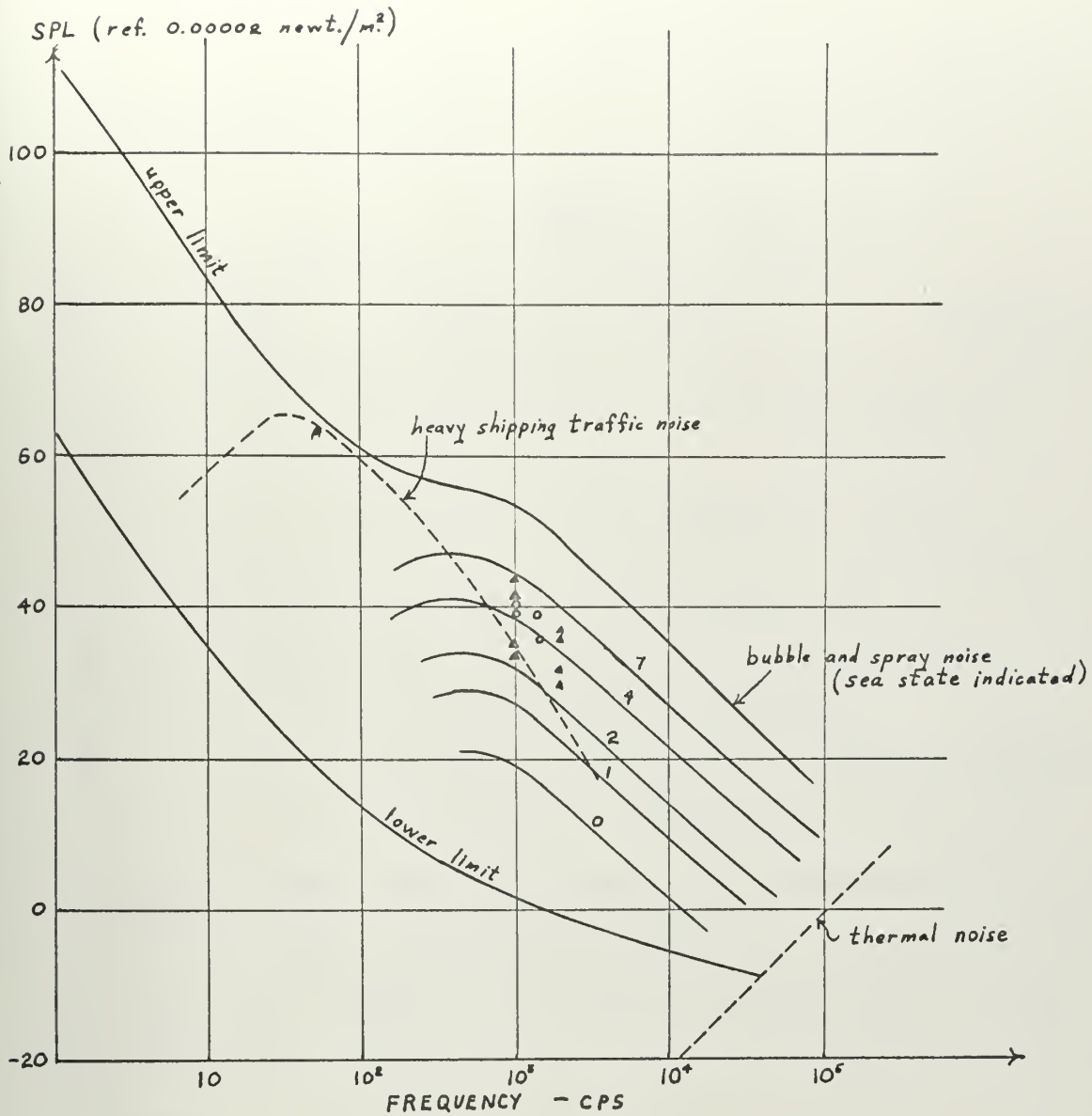


Figure 8. Ambient noise in the ocean(13). Specific shallow water data indicated as follows:

- ▲ (15)
- (16)

about fifteen knots, cavitation noise can become much greater than the ambient noise.

Table 1

<u>Sea State</u>	<u>Beaufort wind force</u>	<u>Wind Speed knots (meters/sec.)</u>	<u>Wave Height feet (meters)</u>	<u>Sea Description</u>
2	3	7-10 (3.5- 5.0)	1-2 (.3- .6)	Scattered whitecaps
3	4	11-16 (5.5- 8.0)	2-6 (.6-1.8)	Frequent whitecaps
4	5	17-21 (8.5-11.0)	5-10 (1.5-3.0)	Many whitecaps
5	6	22-27 (11.5-14.0)	8-17 (2.5-5.0)	Whitecaps everywhere
6	7	28-33 (14.5-17.0)	12-26 (3.5-8.0)	Heaped up sea, blown spray

5. Source Power. The output power of a transducer is limited by cavitation and acoustic non-linearity. Cavitation occurs when the local pressure at or near the transducer is less than the vapor pressure of the water. A sample calculation in Appendix B shows that this limits the transducer to a sound pressure level of 195 db (ref. 0.00002 newt./m²) at a transducer depth of twenty feet.

The source level of the transducer is limited by the approximations required to obtain the acoustic wave equations from the equations of fluid dynamics. The governing approximation comes from the following total derivative (17):

$$\frac{du}{dt} = \frac{\partial u}{\partial t} + \frac{u \partial u}{\partial r}$$

u = fluid velocity vector

t = time

r = fluid particle position vector

If the second term on the right can be neglected, then the wave equation can be satisfied. This is worked out in Appendix B for spherical waves. The result is that the sound pressure level at one meter radius must be less than 254 db (ref. 0.00002 newt./m²).

6. Random Process Channel Model. An input-output relation for the hydroacoustic channel will now be developed. The parameters which will be considered are: signal energy, noise energy, frequency dispersion, time dispersion, and multipath reception.

Since the ambient sea noise is due to a large number of small sources, it will be assumed to be a zero mean, Gaussian random process with spectral density N_f . N_f is then the noise energy density. This noise is independent of the message sent. Therefore the received signal will be a message filtered by the channel plus additive Gaussian noise.

This channel filter function is unknown however. To arrive at a channel description, two assumptions will be made. First, along any given transmission path, the channel is a pure attenuator. Second, the receiver receives the signal over a large number of paths, with the received phase for each path being a uniformly distributed random variable.

Wozencraft and Jacobs show that this description leads to a random process channel model, with the following input-output relationships (18):

$$s(t) = m(t) \sqrt{2} \cos \omega_0 t \quad \text{input}$$

$$r(t) = a(t)m(t) \sqrt{2} \cos (\omega_0 t - \theta) + n(t) \quad \text{output}$$

in which

$$p(a) = 2ae^{-a^2} \quad a \geq 0$$

$$p(\theta) = \frac{1}{2\pi} \quad 0 \leq \theta < 2\pi$$

The amplitude $a(t)$ is thus a Rayleigh-distributed random variable. Experimental data verifies this model in many instances, but other distributions have also been observed (19,20). For the work to follow, $a(t)$ will be assumed to be Rayleigh-distributed.

Before a communications system can be developed, frequency and time dispersion must be discussed. Frequency dispersion will limit the baud length. Experimental data shows that in general, for ranges of interest, frequency dispersion is less than 2 cps (21). It is expected that the system will use a baud corresponding to a much larger bandwidth than this.

Time dispersion of a signal is the range of delays observed over paths of different length. It limits the rate at which signals may be sent over conventional systems. There is very little experimental data on shallow water time dispersion. The calculations in Appendix C show that about

1/5 second is the longest time that need to be considered, at a range of fifty miles. This is about 40 percent of the dispersion for the SOFAR channel which is severely limited in this respect (22), and it corresponds to an experimental value observed in the Florida Straits (23).

Part II
COMMUNICATIONS SYSTEM

1. Frequency Selection. The optimum frequency is the one which allows the greatest bandwidth and the signal to noise ratio. Neglecting the noise, low frequencies are the best. Spreading losses are about the same for all frequencies. For a state 3 sea, surface reflection losses are 0.5 db./bounce at 800 cps, 0.95 db./bounce at 1000 cps, and 2.0 db./bounce at 1500 cps. This becomes worse for higher frequencies or higher seas. Attenuation also increases with frequency and is first significant for the fifty mile range at about 2000 cps. Therefore, primarily because of surface losses, an upper limit of 1.5 kc will be used. A lower limit of 800 cps will be used. At low frequencies it is possible to get strong harmonics from shipboard machinery. This is generally worst at about 500 cps. One prime example of low frequency noise is propeller harmonics which may be very strong.

A plot of noise and fifty mile signal strength is shown in figure 9 as a function of frequency. This plot uses the same data as figures 7 and 8. A noise level corrected to a 10 cps bandwidth is also shown. This is sufficient for the correlation time of $1/6$ second which will tentatively be used. Experiments show that at long ranges, the signal will remain about 80% coherent by autocorrelation for up to $1/4$ second (23).

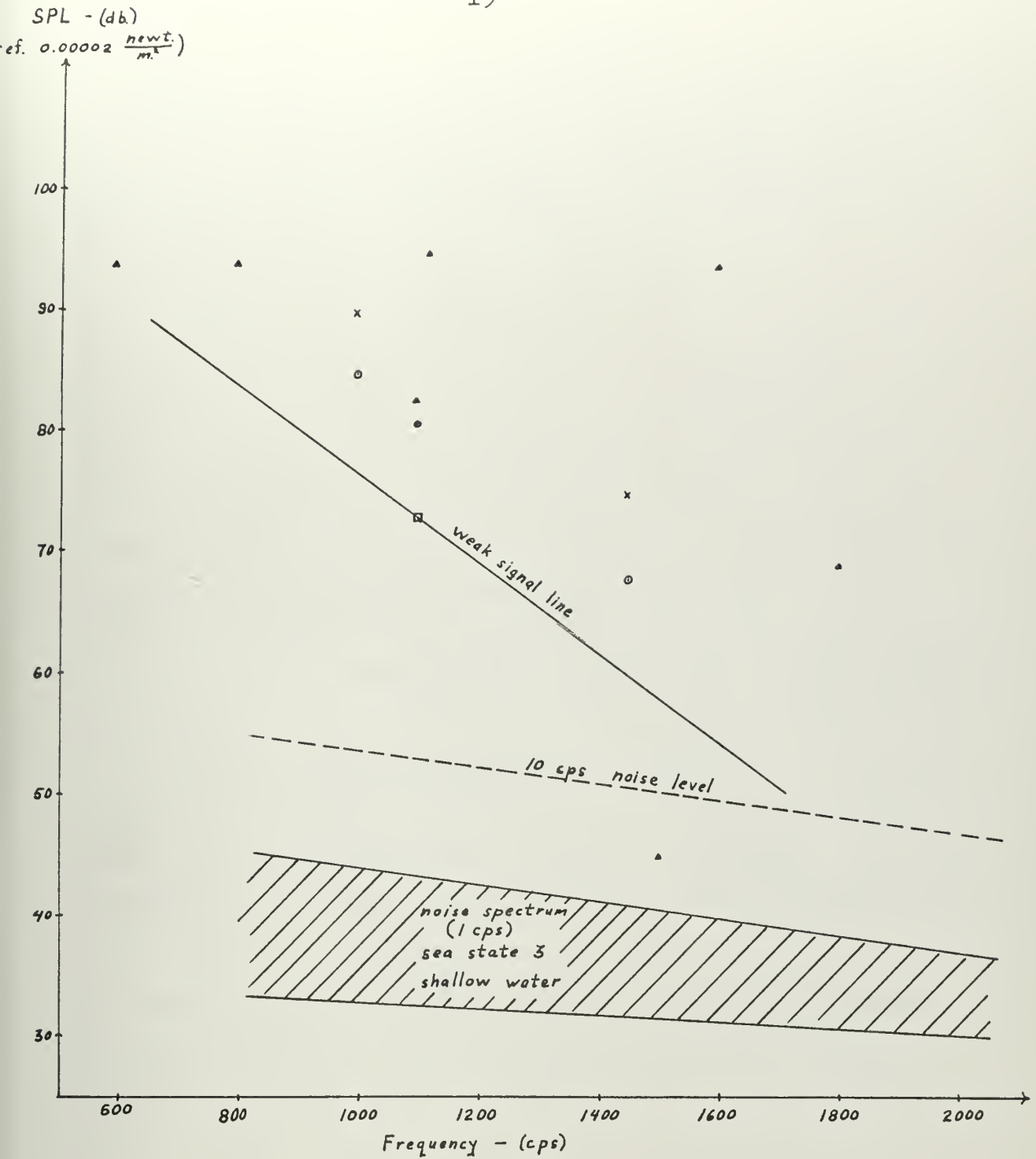


Figure 9. Expected signal-noise separation in a state 3 sea. (See figures 7 and 8.)

2. Binary Signalling. A simple binary communications system will now be developed for the shallow water channel. The signal set will be an orthogonal pair of cosine waves, as follows:

$$s_0(t) = \sqrt{2} \cos \omega_0 t$$

$$s_1(t) = \sqrt{2} \cos \omega_1 t$$

This set is considered the easiest to use for this system. Signals which are time orthogonal are not well suited to this channel since the time of arrival is unknown. Since both phase and amplitude are random processes, neither phase nor amplitude modulation was considered suitable.

When the signal $s_0(t)$ is sent, the received signal is of the form:

$$r(t) = \sum_{i=1}^N a_i \cos(\omega_0 t + \theta_i) + n(t)$$

where the i 's represent the different multipaths. As noted in Part I, this leads to the following random process model:

$$r(t) = a(t) \cos(\omega_0 t + \theta) + n(t)$$

in which a and θ are random variables with the following probability density functions at any instant of time:

$$p(a) = 2a e^{-a^2} \quad 0 \leq a$$

$$p(\theta) = 1/2\pi \quad 0 \leq \theta \leq 2\pi$$

This model and the following assumptions will be used to arrive at a suitable binary receiver:

a. $a(t)$ and $\theta(t)$ are constant over the signal interval T , but vary randomly from interval to interval.

b. $n(t)$ is a white Gaussian noise random process, of spectral density N_0 , and it is independent of the signal.

c. The two signals, $s_0(t)$ and $s_1(t)$ have equal energy and are equiprobable.

d. There is no intersymbol interference.

A maximum likelihood receiver will be used. For this receiver, that message is selected for which the probability of the received signal conditioned by the messages is highest. The details of this receiver have been worked out by Turin (26), and for more general time-varying cases by Kailath (27) and Price (28). In the case of the narrow band signals chosen for the signal set, the receiver was determined to be a device which correlates, squares, and sums the quadrature components before making a decision. The correlation receiver is shown schematically in figure 10. Figure 11 is an envelope detector receiver which can be shown to be essentially the same.

The correlation receiver can be explained heuristically by a geometric argument. The quadrature noise components of the received waveform are zero mean Gaussian random variables of variance $N_0/2$, where N_0 is the mean square noise power. The quadrature signal components of the received waveform are also zero mean Gaussian random variables, but with a variance of $E_0/2$, where E_0 is the mean square signal power. If a signal is present the received quadrature com-

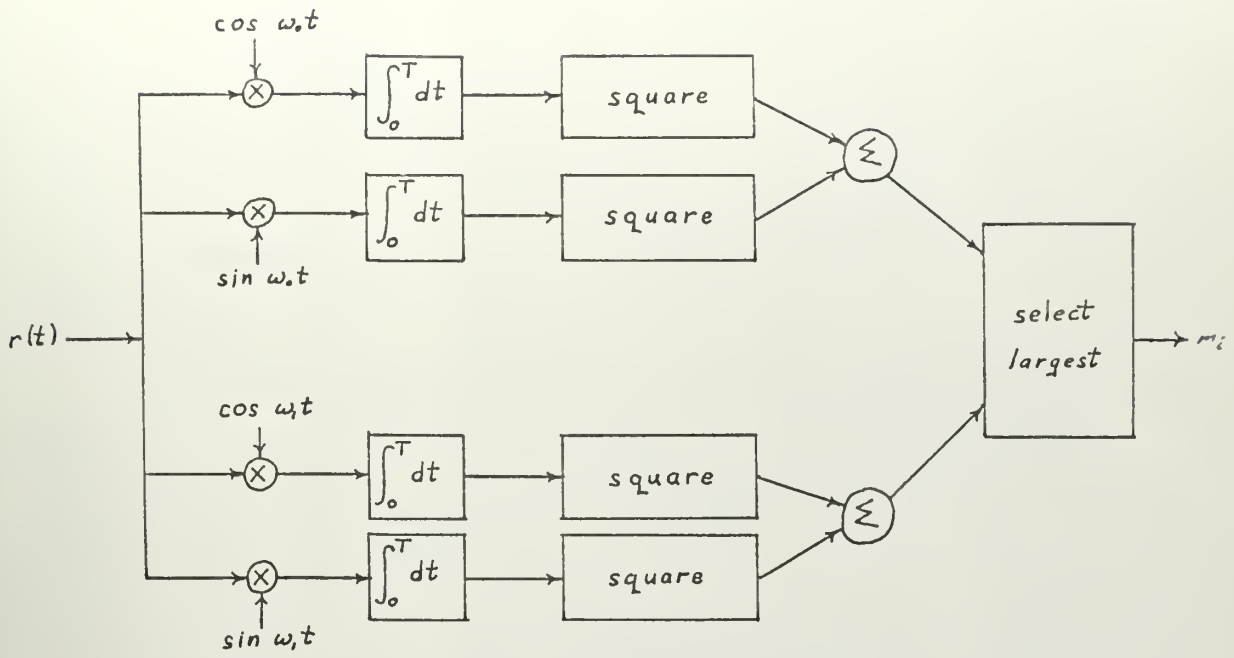


Figure 10. Binary correlation receiver.

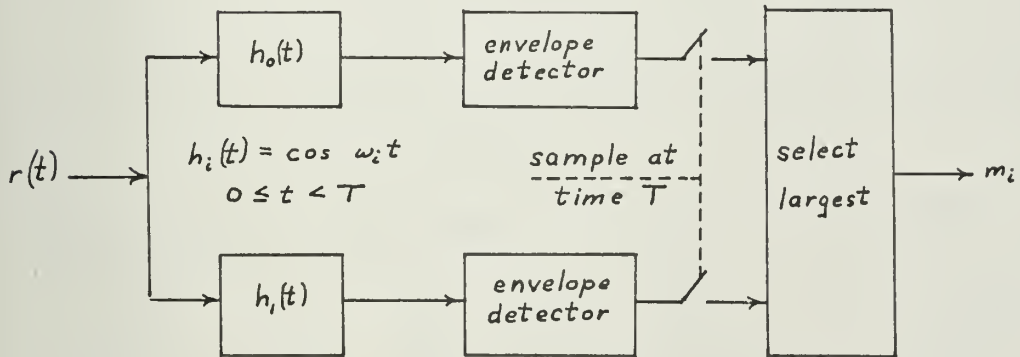


Figure 11. Binary envelope detector receiver.

ponents are therefore zero mean Gaussian random variables with variance $\frac{E_s + N_s}{2}$. These Gaussian random variables are illustrated in figure 12, in the s_o -plane and the s_i -plane for the case when $s_o(t)$ is sent. In each case the amplitude of the resultant vector is a Rayleigh distributed random variable.

The error probabilities for the likelihood receiver are developed in Wozencraft and Jacobs (29), by computing it first for the random phase case only, to obtain:

$$P(\mathcal{E}) = \frac{1}{2} e^{-E/2N}$$

Averaging this error over a Rayleigh amplitude distribution, the following error probability is obtained for the random phase and random amplitude channel:

$$P(\mathcal{E}) = \frac{1}{2 + E/N}$$

Using this formula, the efficiency of the simple binary channel may now be determined. Referring to figure 9, with a 10 cps bandwidth and the weak signal line, table 2 summarizes the binary channel error probability at various frequencies.

Table 2

<u>Frequency</u>	<u>E/N (db.)</u>	<u>E/N</u>	<u>P(\mathcal{E})</u>
800	29	790	0.0013
1000	23	200	0.0050
1250	15	31.5	0.030
1500	8	6.3	0.12

3. Channel Capacity and Coding. In 1948, C.E. Shannon showed that whenever signals are transmitted at some rate, R , less than channel capacity, C , then an arbitrarily small error rate can be achieved by coding with a sufficiently

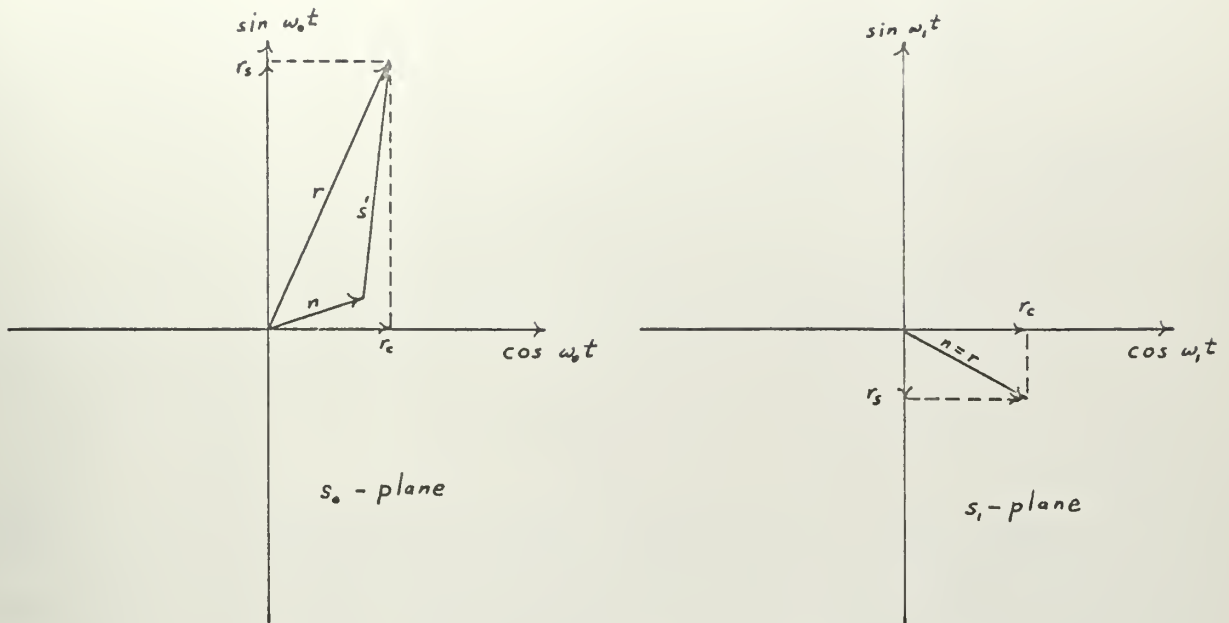


Figure 12. Received signal in the s_o -plane and s_i -plane when message $s_o(t)$ is sent.

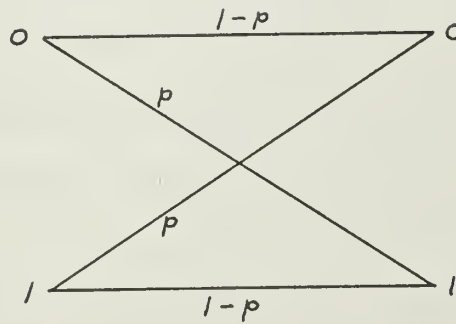


Figure 12A. The binary symmetric channel.

long block length (30). For the binary symmetric channel with crossover probability p , as shown in figure 12A, the channel capacity has the rather simple form (31):

$$C = 1/T \left[1 + p \log_2 p + (1-p) \log_2 (1-p) \right] \text{ bits per second}$$

where T is the signal time required to achieve p . It can also be shown that for n arbitrary channels being used in parallel, the capacity is:

$$C = \sum_{i=1}^n C_i$$

where C_i are the individual channel capacities. This last formula holds for simple parallel use in which a decision is made on each channel. If the decision is made on the collective output probabilities of the individual channels, then the channel capacity is somewhat greater, since in the first method some information is lost by the intermediate decision.

A sixty word per minute data rate requires approximately thirty bits of information per second. If an average channel capacity of five bits per second can be obtained, then a minimum of six channels are required for effective transmission. At transmission rates very close to capacity however, very elaborate coding schemes are required to achieve a reliable transmission. In general, it can be shown that for proper coding the probability of error is bounded by functions of the transmission rate (32):

$$e^{-n(E_L(R) + O(n))} \leq P(\mathcal{E}) \leq e^{-nE(R)}$$

where $E_L(R)$ and $E(R)$ depend on the channel, and n is the code

block length. For rates less than channel capacity, both $E_L(R)$ and $E(R)$ are positive. These functions will not be evaluated for this channel.

For this fading channel, the rate is limited by the number of parallel channels. The signal interval cannot be shortened to much less than one sixth of a second because of intersymbol interference. The number of channels is limited by the useable frequency band. Above about 1500 cps, very little capacity is gained for the addition of an extra channel. Assuming a signal interval of one sixth of a second, and transmitting five information bits during each interval, the effect on the rate as a function of capacity of adding more channels is summarized in table 3, and figure 13. A minimum useable frequency of 900 cps and a frequency separation of 20 cps was assumed.

Table 3*

<u>Channel #</u>	<u>frequencies</u>	<u>P(ϵ)</u>	<u>ΔC</u>	<u>C</u>	<u>R/C</u>
1	900 & 920	.0028	5.8		
2	940 & 960	.0040	5.8		
3	980 & 1000	.0057	5.7		
4	1020 & 1040	.0076	5.6		
5	1060 & 1080	.0100	5.5	28.4	1.06
6	1100 & 1120	.0124	5.4	33.8	.89
7	1140 & 1160	.0154	5.3	39.1	.77
8	1180 & 1200	.0213	5.1	44.2	.68
9	1220 & 1240	.0263	4.9	49.1	.61
10	1260 & 1280	.0333	4.7	53.8	.56
11	1300 & 1320	.0408	4.5	58.3	.51
12	1340 & 1360	.0562	4.1	62.4	.48
13	1380 & 1400	.0685	3.8	66.2	.45
14	1420 & 1440	.0918	3.3	69.5	.43
15	1460 & 1480	.114	2.9	72.4	.41

* Based on a power level allowing ten channels. For less channels P(ϵ) is better, for more worse (See Part I).

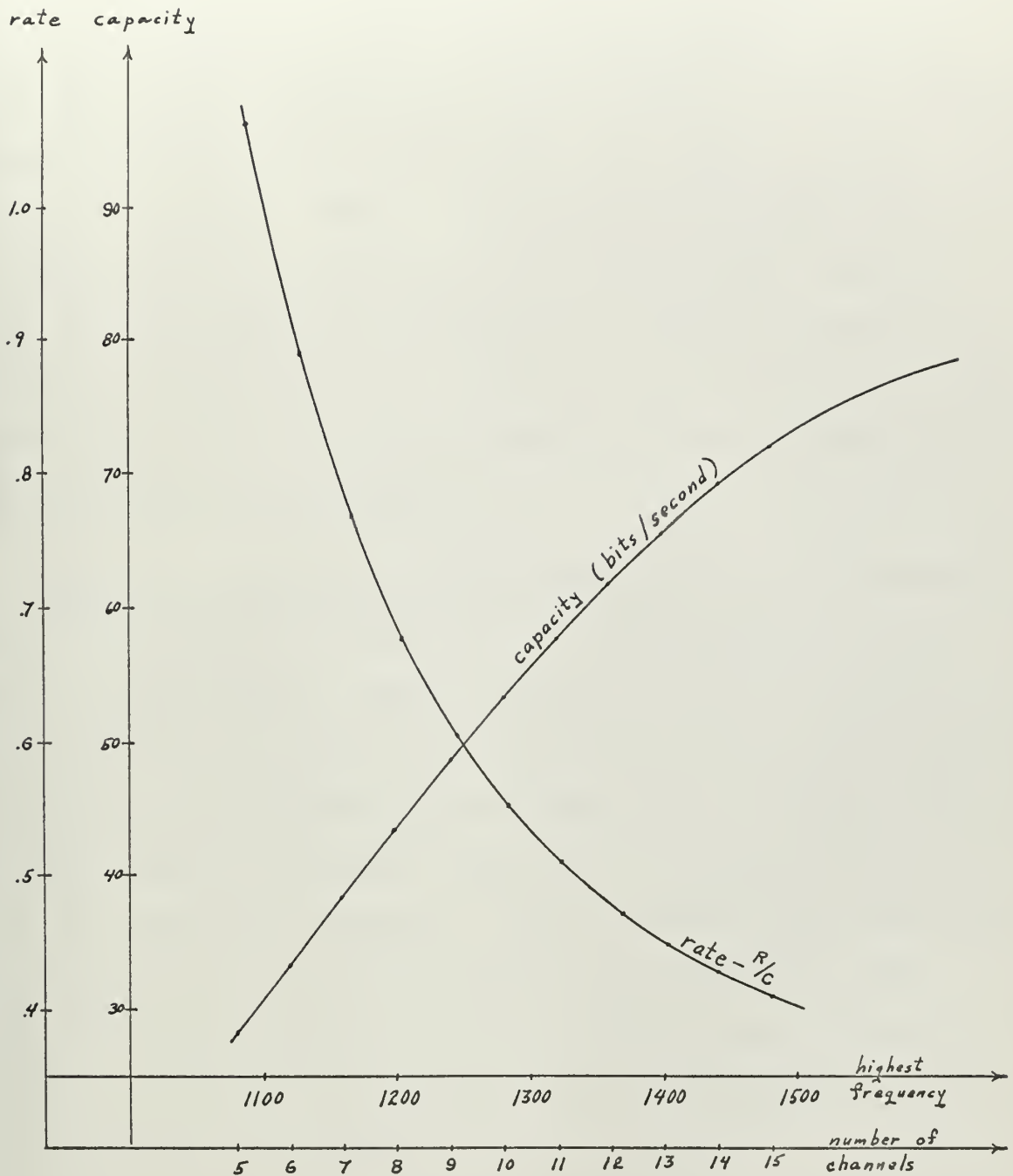


Figure 13. The effect of adding additional higher frequency channels on capacity and rate. (Transmission at 30 bits per second.)

There are several interesting methods of coding and decoding which will be discussed after developing a communications system for the hydroacoustic channel. In the next section, the system will be developed first using simple transmission and then diversity and block coding. Block coding is taking a block of input digits and coding them into a longer group of coded digits for transmission. The error will be calculated for a decoder which makes an intermediate decision on each bit. As noted this is not the most efficient use of the channel, but it is considerably easier for decoding and for error calculations.

4. Representative Communications Systems. A simple system which can transmit the necessary 30 bits per second is composed of five parallel binary channels. Each one sixth of a second, a five bit symbol is transmitted, one bit per channel. To avoid shipping noise a minimum frequency of 900 cps will be used. Table 4 lists the individual crossover probabilities for these five channels. The orthogonal signal pair are 12 cps apart to allow a $1/6$ second signal interval. The channels are separated by 20 cps, to permit easier tuning, in case of a doppler shift which could be as high as 15 cps for two ships at 15 knots.

Table 4

<u>Channel #</u>	<u>frequencies</u>	<u>P(E)</u>
1	900 & 912	0.0014
2	932 & 944	0.0019
3	964 & 976	0.0024
4	996 & 1008	0.0030
5	1028 & 1040	0.0038

The error rate per five bit symbol for this transmission system can easily be computed as:

$$P(\mathcal{E}) = 1 - P(\text{no bit errors})$$

For independent bit errors the error probability is easily computed to be 0.013 per five bit symbol. Due to receiver imperfections, and variation of the channel from the model which will be discussed in the next section, this can only be considered an order of magnitude. Therefore, methods of improving the reliability will be investigated. Shannon's coding theorem discussed in the last section indicates that the error rate may be improved without an increase of power.

The easiest method to implement for this channel is not normally thought of as coding, though it is in reality a simple code. This is frequency diversity. For illustration fifteen parallel channels will be used, with each bit being transmitted over three channels instead of one. To maintain the same transmitter power, each channel will use only one third of the power as for the simple system binary channels. The error probabilities for the fifteen channels are listed in table 5. The frequencies are spaced as for the simple five channel system.

Table 5

<u>Channel #</u>	<u>P(\mathcal{E})</u>	<u>Channel #</u>	<u>P(\mathcal{E})</u>
1	.0025	9	.0264
2	.0059	10	.0324
3	.0074	11	.0385
4	.0090	12	.0446
5	.0117	13	.0550
6	.0149	14	.0705
7	.0184	15	.0840
8	.0224		

A block diagram of the triple diversity receiver is shown in figure 14. The w_i are weighting functions which depend on the signal-noise ratio for the particular binary channel (33):

$$w_i = \frac{E_i/N_i}{1+E_i/N_i}$$

For the fifteen channels being used, they range from 0.99 for channel number one to 0.86 for channel number fifteen. For a simple equal energy L-fold diversity system the error probability can be computed from the following formula (34):

$$P(\epsilon) = p^L \sum_{j=0}^{L-1} \binom{L+j-1}{j} (1-p)^j$$

This is plotted for L equal to 1, 2, and 3 in figure 15. As an example, if p is 0.04, three-fold diversity yields a bit error probability of 0.00065. For a five bit symbol this would become an error rate of 0.0033. Assuming that p equal to .04 is a good average from table 5, this is a four times improvement over simple five channel transmission. A general error calculation method for unequal energy and noise on the different diversity channels is worked out in Appendix D.

If data is to be transmitted with an accuracy better than this diversity system, coding will be required. One method, block to block coding will be discussed now. Other methods will be compared to it in the next section. A practical block to block coding system is the parity check code. For illustration, each five bit symbol will be encoded into a fifteen bit code word. The first five bits of the code word are the five information bits; the remainder are modulo two

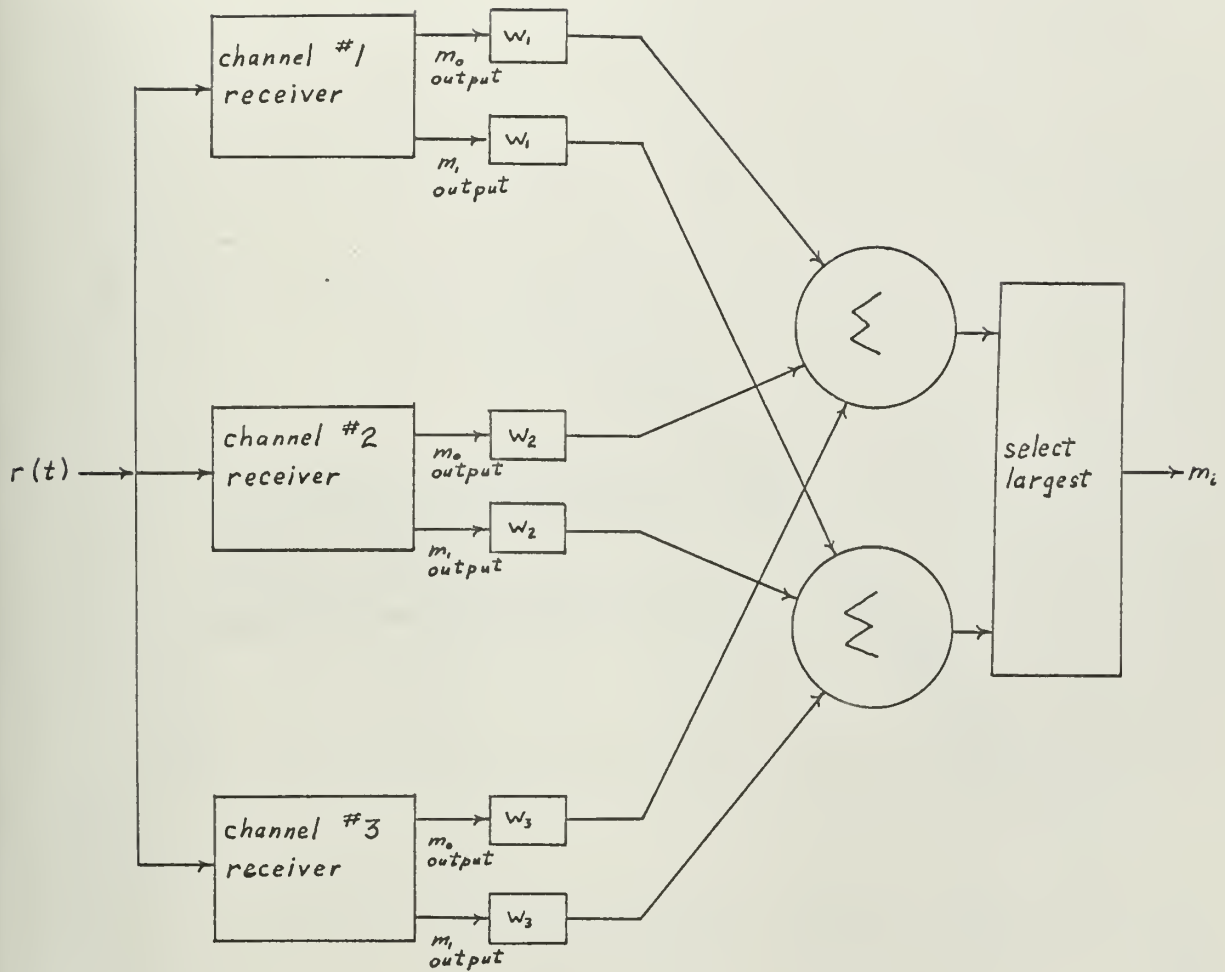


Figure 14. Three-fold diversity receiver.

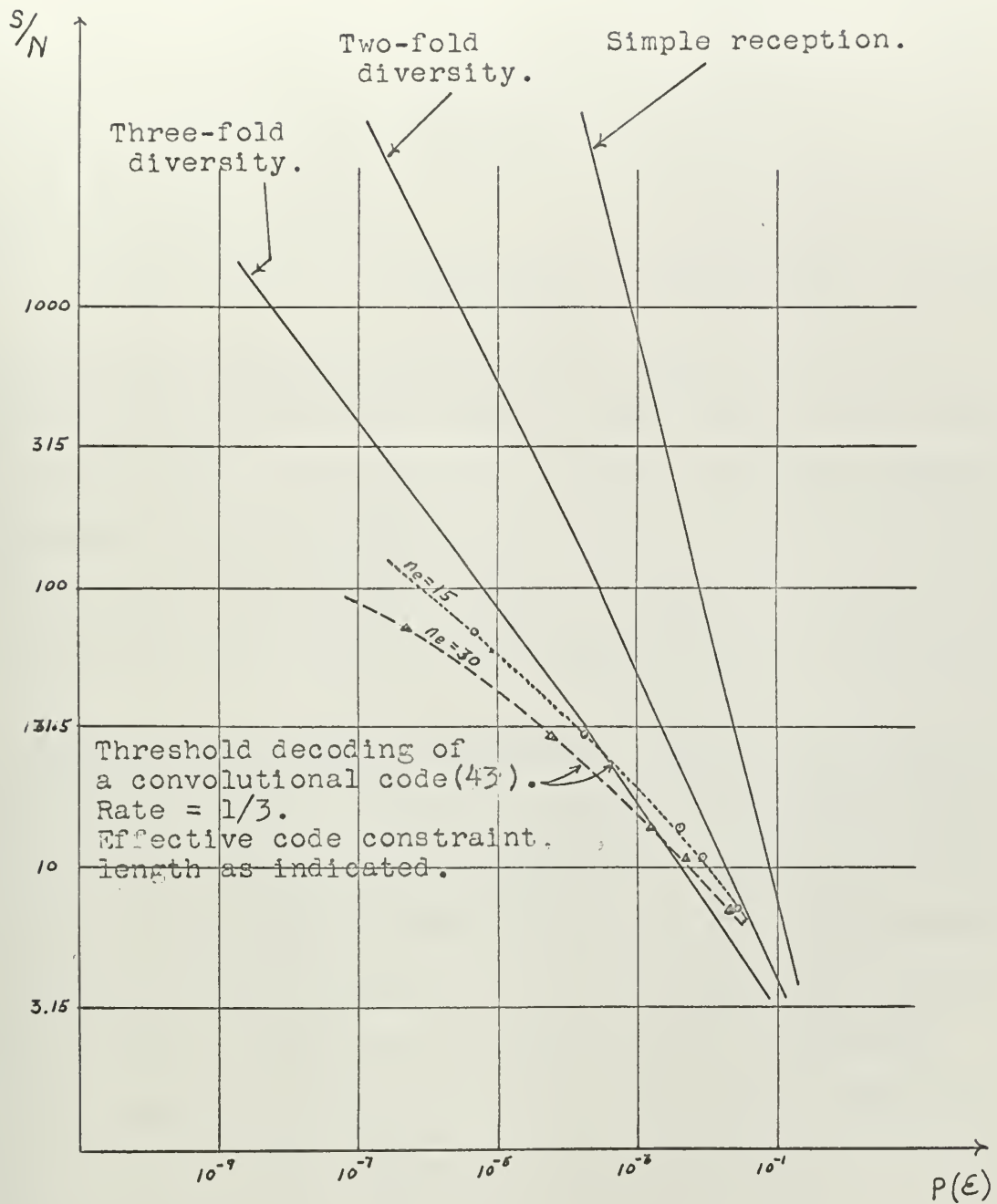


Figure 15. Binary receiver error probabilities for the Rayleigh fading channel.

sums of several of these five bits. Proper selection of the code, and use of an appropriate receiver, will permit correction of any three bit or lesser error in the reception of the fifteen bit code word (35). For this code the error probability then becomes:

$$P() = 1 - p(\text{no errors}) - p(\text{one error}) - p(\text{two errors}) - p(\text{three errors})$$

Carrying out this calculation for the data of table 5, the error probability is approximately 0.004 per five bit symbol, or approximately the same as for triple diversity. Further improvement can be accomplished by coding by use of a longer block length, for example, coding two five bit symbols into a thirty bit code word, or three symbols into a 45 bit word.

5. Suitability of Coding Techniques. In the last section simple transmission, frequency diversity and a short block length parity check code were compared. There was a significantly smaller error using diversity or the coding scheme. To achieve a still smaller error probability, much larger block length or other types of codes would be required. Various coding techniques will now be discussed, which may be used if the added complexity can be justified by the improved performance.

A block to block parity check code was used as an example in the last section. For this type of coding system, the number of computations required by the decoder increases roughly as the cube of the block length (36), and as noted,

only specific error combinations can be corrected. This limits its capability of correcting a large burst of errors, except for very long codes. In general, block code receivers make a decision on each bit before decoding. This means that the confidence level in each bit is lost. The performance can be improved by finer quantization in the receiver before decoding. It can be shown, however, that three level quantization will achieve half of the possible improvement, and that finer quantization than this gives an increasing small improvement (37). Three level quantization is best described by the binary erasure channel shown in figure 16. For this channel the bias level must be properly set so that both p and q are small, where p is the crossover probability, and q is the erasure probability. This type of channel is more difficult to instrument than the simple binary channel and has not been used as extensively (38).

Some of the drawbacks of block to block coding may be met with convolutional codes (39). A simple encoder is shown in figure 17 (40). Each transmission interval, v parity checks on a k bit register are transmitted. Between intervals, one bit is moved out of the k bit register on the right, and one new information bit is moved in at the left. Each information bit is in the transmission sequence for k intervals, and there are an average of v transmitted bits per information bit. Since at least five information bits must be transmitted on fifteen channels six times per second, v is

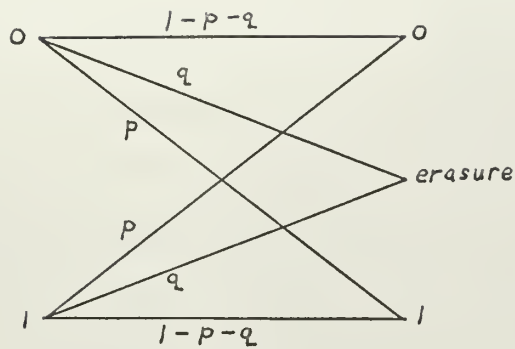


Figure 16. The binary erasure channel.

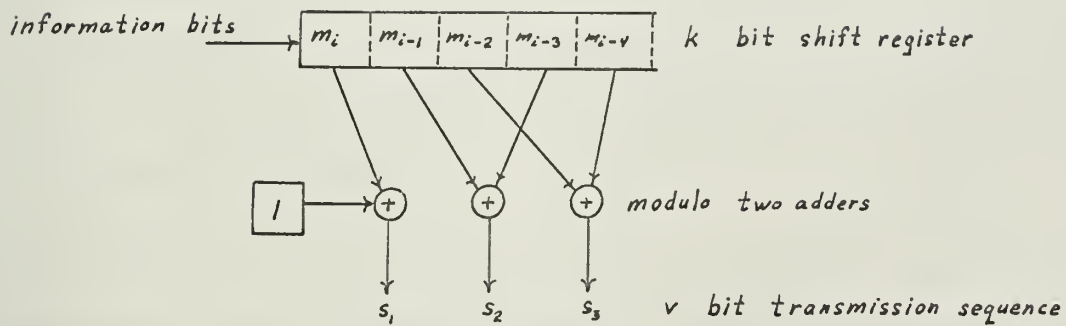


Figure 17. Convolutional encoder.

limited to three for the channel being described.

Two good decoding schemes are known for convolutional codes: sequential decoding (41), and threshold decoding (42). In the former an n bit message is treated as a tree with n sequential nodes. A very good reliability can be achieved if a computer with a large enough memory to backtrack through many paths along the tree is used. This may be 2^{10} bits or more (39). Once an error is made because backtracking is no longer possible, a large block of errors may be made. This is satisfactory in a feedback system where repeats may be requested. Since the transmission time over a fifty mile hydroacoustic channel is approximately a minute, this type of channel is best suited for broadcast or prearranged time sharing, with little or no possible feedback. A simpler decoding scheme for convolutional codes which avoids these block errors at the expense of a higher average error rate is threshold decoding.

The threshold decoder uses only shift registers, modulo two adders, and a threshold device. For good results each bit must remain in the register for more than one fifteen bit transmission time, since for this short coding length the results are about the same as for triple diversity as noted on figure 15 (43). For short block lengths, the results with threshold decoding on a convolutional code are somewhat better than for block to block coding, with no more complexity. This is because it can take advantage of the a posteriori probabilities in the binary channels.

Part III
DISCUSSION

1. General. In this section the assumptions leading to the channel model and the resulting communications system will be discussed first. The importance of the assumptions to the resulting communications system, and their expected variations will be brought out. Next the hydroacoustic conditions in various ocean areas at different times of the year will be discussed.

2. Assumptions. The most important assumptions made in the preceding development have been the following:

- a. There is no intersymbol interference.
- b. The multipath reception produces a Rayleigh amplitude distribution.
- c. During each signal interval, the received phase and amplitude are constant.
- d. The receiver is synchronized to the transmission interval.
- e. The noise is white and Gaussian.
- f. Errors on different binary channels are independent.

Assumptions a., c., and d. are related. To minimize intersymbol interference, the signalling interval must be long enough for most of the energy transmitted during a given interval to be received during an equal delayed interval at the receiver. The time used is based on the calculation in appendix C. The intersymbol interference can be treated as

an additional noise component which increases the crossover probability, or if it can be estimated, used in a receiver with memory. By making the signalling interval long enough for intersymbol interference to be negligible, the interval may become too long to assume a constant phase and amplitude during the interval. This problem can be corrected by using time diversity reception during each signal interval. Since a small amount of intersymbol interference is unavoidable, and also because the transmission time between the terminals will vary, it will be impossible to obtain perfect synchronization at the receiver. Range changes may be corrected by a doppler circuit. Transmission path variations should be fairly small so that the time variations due to this phenomena will be small compared to the signal interval. In this case these variations are also correctable. In summary, these assumptions can be met as well as desired by proper selection of the signalling interval and the use of time diversity reception if required.

Experimental data indicates that the Rayleigh amplitude distribution is a good assumption much of the time, but that it may differ (19,20). For long ranges these differences are most evident in the higher moments, and do not differ significantly in the mean or mean square. At short ranges only a few paths may be of interest, and in this case the distribution is more favorable than a Rayleigh distribution (19). Figure 18 compares a typical short range amplitude distribution with the Rayleigh distribution.

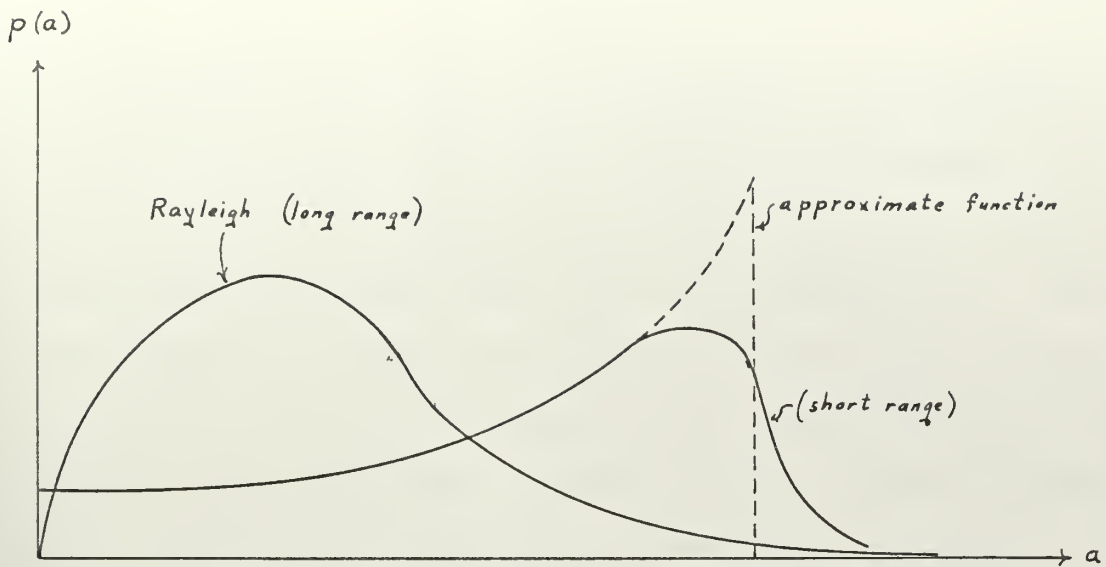


Figure 18. Typical amplitude distributions.

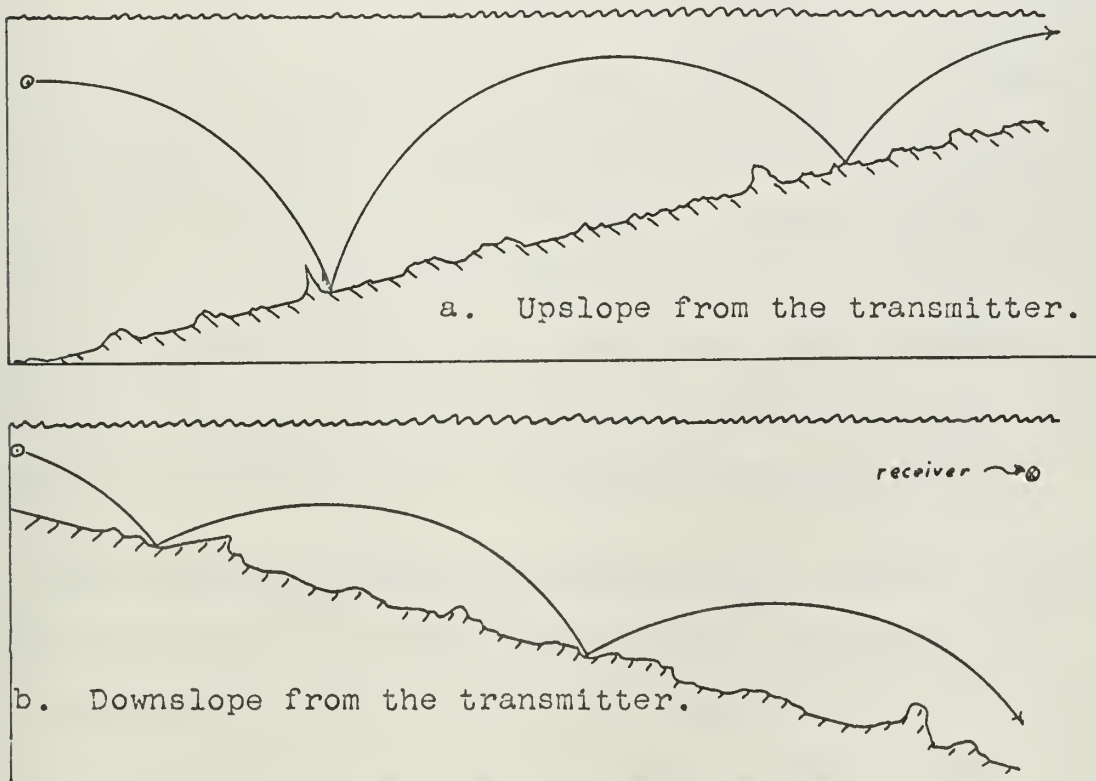


Figure 19. Effect of a sloping bottom on communications via the bottom reflection channel in shallow water.

Although most ambient sea noise can be considered white and Gaussian for the narrow band binary channels, other forms of noise may be present. Rotating machinery harmonics, or marine life may affect only one or two frequencies. Most of these noises are most severe under 1000 cps, but a source on a receiving ship is potentially dangerous. A careful noise analysis of potential receiving vehicles will permit optimum frequency selection with respect to the noises. Impulse noises may also be present. These can be minimized by clipping the signal at a level which depends on the average impulse noise power and the expected signal levels.

In arriving at $\frac{1}{2}$ system error probabilities, errors were considered independent of other channels. If these binary errors are not independent, then the resulting system error probabilities will be different. If for example the errors on two of three diversity receivers are correlated, the resulting bit error is only about as good as double and not triple diversity. No good data is available on how closely correlated transmission over adjacent frequencies is.

3. Ocean Conditions and the Channel Model. Several factors affect the prevailing ocean hydroacoustic conditions (40). The temperature, and hence the vertical profile of the velocity of sound vary with both latitude and time of year, and in some cases the time of the day. The depth of the water and the bottom profile affect bottom reflection transmission. Weather conditions affect both noise and surface reflection

losses. All the calculations made have been for a moderate, state three, sea. Heavier weather conditions reduce the reliability considerably.

Surface trapped channels occur only when the water temperature is isothermal or perhaps increasing with depth. This condition is somewhat unstable and can occur only when the surface waters are being cooled. Experimental data indicates that these conditions exist most of the year in polar regions, during winter in mid-latitudes, and only rarely in tropical waters. In mid-latitudes the layer depth will be from 1000 feet to 1500 feet in the winter, but a sharp thermocline will exist near the surface in the summer. Since water depth is not important to the surface channel, the model developed will apply to all high latitude ocean areas in the winter, but only to shallow water, or polar waters during the summer months.

The bottom reflection channel can also be quite variable as to results. For any given depth, the bottom slope is quite important, as is illustrated in figure 19.

Part IV

CONCLUSIONS AND RECOMMENDATIONS

1. Conclusions. In Part I it was shown that the signal-noise ratio for the surface channel and the shallow water bottom reflection channel could be estimated. It was further shown that the appropriate model was a Gaussian random process, in which the received signal had a Rayleigh amplitude distribution and unknown phase with additive white Gaussian noise. Using this model an appropriate binary receiver was found to be a quadrature correlation device. A combination of five of these receivers could be used to send data at 60 wpm with a moderate error rate. Improvement in the error rate was best obtained by frequency diversity, and could be further improved by coding at the expense of complexity and cost. In Part III, it was shown that the model was reasonable for shallow water any time if the bottom did not slope away from the transmitter too fast, for mid-latitudes in the winter, and for polar regions most of the year. These results are applicable for moderate weather conditions, and ranges of up to fifty miles.

2. Recommendations. Although the basic form of the receiver could be developed, the actual parameters could only be estimated. A better understanding of these parameters is needed for the actual development of a suitable system. Some items of interest which warrant additional experimental

research are the following:

- a. the noise spectrum of potential receiving vehicles.
- b. the range and distribution of multipath time delays for various channels.
- c. the length of time during which phase and amplitude of a multipath signal will remain coherent.
- d. the correlation of errors on binary channels of adjacent frequency.

APPENDIX A

1. Surface Channel Sample Calculations.

For these calculations the following assumptions will be made:

Isothermal water with a velocity gradient of 0.0052 m./sec./m.

Frequency ... 1 kc.

Range ... 50 miles.

Layer depth ... 30.5 meters.

Sea state ... 3

Source ... 185 db (ref. 0.00002 newt./m.) at 1/4 m. radius. This is 173 db at a 1 meter radius.

$$a. \quad R = \frac{c_o}{a \cos \theta_o} (\sin \theta_o - \sin \theta)$$

$$\theta = 0$$

$$c_o = 1500 \text{ m/sec.}$$

$$a = 0.0052 \text{ m/sec/m.}$$

$$Y = 30.5 \text{ m}$$

$$\cos \theta_o = \frac{c_o}{c_o + aY} \approx \frac{1 - \theta_o^2}{2}$$

$$\theta_o = 0.0152 \text{ radians} = 0.87 \text{ degrees}$$

$$R = 4380 \text{ meters}$$

b. Spherical spreading loss.

$$L = 20 \log_{10} R/2 = 20 \log_{10} 2190 = 67 \text{ db.}$$

c. Cylindrical spreading loss.

$$L = 10 \log_{10} \frac{50 \text{ miles}}{R/2} = 10 \log 36.7 = 15.7 \text{ db.}$$

d. Surface reflection loss.

$$\text{Number reflections} = \frac{50 \text{ miles}}{2R} = 9.2$$

Number reflections = 10

Loss per bounce = 0.95 db for a 4 foot wave height

$L = 0.95 \times 10 = 9.5 \text{ db.}$

- e. Absorption. Negligible for this range and frequency.
- f. Total losses. $67 + 15.7 + 9.5 = 92 \text{ db.}$
- g. Signal level. $173 - 92 = 81 \text{ db (ref. 0.00002 newt./m.)}$

2. Bottom Reflection Channel Calculations.

The same assumptions are made as for the surface channel except there is no layer, and:

Water depth ... 300 meters, flat bottom.

Velocity gradient ... 0.075 m./sec/m.

a. $R = \frac{c_0}{a \cos \theta_0} (\sin \theta_0)$

$R = 3500 \text{ meters}$

b. Spherical loss.

$L = 20 \log_{10} 3500 = 71 \text{ db.}$

c. Cylindrical loss.

$L = 10 \log_{10} \frac{50 \text{ miles}}{3500} = 10 \log_{10} 23 = 13.6 \text{ db.}$

d. Bottom Loss.

Number reflections = $\frac{50 \text{ miles}}{2R} = 11.5$

Number reflections = 12

$L = 12 \times 0.3 = 3.6 \text{ db.}$

e. Surface loss.

$L = 12 \times 0.95 = 11.4 \text{ db.}$

f. Total loss. $71 + 13.6 + 3.6 + 11.4 = 100 \text{ db.}$

g. Signal level . $173 - 100 = 73 \text{ db. (ref. 0.00002 newt./m.)}$

APPENDIX B

1. Cavitation.

Cavitation occurs when the acoustic pressure plus the ambient pressure is less than the vapor pressure of water. The following numerical values will be used in this calculation:

vapor pressure = 0.6 psi at 85 degrees F. (decreases with T)

atmospheric pressure ... 14.7 psi

water depth = 20 feet

a. Static pressure.

$$p = 14.7 + 0.444 \times 20 = 23.5 \text{ psi}$$

b. Allowable acoustic pressure.

$$p = 23.5 - 0.6 = 22.9 \text{ psi} = 1.58 \times 10^5 \text{ newt./m}^2$$

c. Sound pressure level.

$$\text{SPL} = 20 \log_{10} p/p(\text{ref})$$

$$p(\text{ref}) = 0.00002 \text{ newt./m}^2$$

$$\text{SPL} = 20 \log_{10} 7.9 \times 10^9 = 198 \text{ db.}$$

Allowing 3 db for peak versus mean square, the SPL is limited to 195 db (ref. 0.00002 newt./m².)

2. Non-Linearity.

For the acoustic approximation we require:

$$\frac{u \partial u}{\partial r} \ll \frac{\partial u}{\partial t}$$

Assuming spherical harmonic waves, the following equations apply:

$$p = \frac{p_0}{r} e^{j(\omega t - kr)}$$

$$u = \left(\frac{1}{r} + jk \right) \frac{p_0}{j\omega \rho} e^{j(\omega t - kr)}$$

Taking the indicated derivatives, we now obtain:

$$\frac{p}{j\epsilon_0} \left[\frac{1}{r^2} + \frac{jk}{r} + k^2 \right] \ll j\omega^2$$

$$\text{let } f_0 = \frac{\omega_0}{2\pi} = 1000 \text{ cps}$$

$$r = 1 \text{ meter}$$

then, since $k = \frac{\omega_0}{c}$, the bracketed term on the left is less than 10. The inequality can be simplified to

$$\frac{p}{\epsilon_0} \ll \omega^2$$

In sea water, $\epsilon_0 \approx 1000 \text{ kg/m.}$

$$\omega^2 = 4\pi^2 \times 10^6 \text{ at } f_0 = 1 \text{ kc.}$$

so that the inequality becomes:

$$p \ll 4\pi^2 \times 10^9$$

Letting $p = 10^8$, we obtain the following sound pressure level:

$$\begin{aligned} \text{SPL} &= 20 \log_{10} p/p(\text{ref}) \\ &= 20 \log_{10} \frac{10^8}{0.00002} = 254 \text{ db (ref. } 0.00002 \text{ newt./m}^2\text{.)} \end{aligned}$$

APPENDIX C

1. Time Dispersion. The maximum difference in the length of time it takes a signal to reach the receiver via two different multipaths limits the rate at which signals may be sent. This difference is due to sound velocity fluctuations, and path length fluctuations. This time difference will now be estimated for the special case of a bottom reflecting channel. Variations will be less severe for surface channels or for shallower water. It will be assumed that the average velocity of sound differs by a maximum of four meters per second over different paths. This corresponds to an average temperature difference of 1.00°F. This is a reasonable value since variations over several miles are normally quite small in open waters. It will further be assumed that the ray paths are straight lines. This is illustrated in figure 20. Since θ is limited to $10^\circ - 15^\circ$ at the bottom for good reflection coefficients, an average value of 6° will be chosen. This is reasonable since the most significant paths are those leaving the transducer within a few degrees of the horizontal. All these paths will reach the bottom at approximately the same angle, so that the average variation will be only about 1° .

Using these values, a range of 50 miles, and a sound velocity of 1500 m/sec., the time variation will now be computed.

$$T = D/V = \text{slant range/velocity}$$

$$R = D \cos \theta = \text{horizontal range}$$

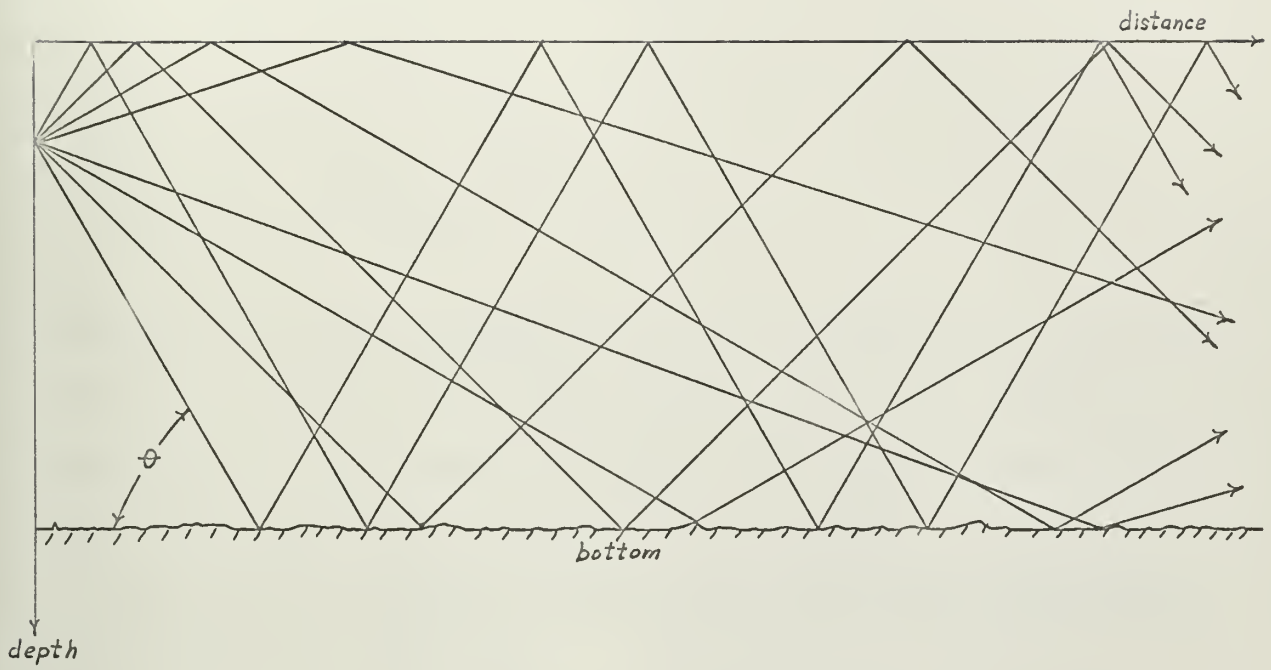


Figure 20. Model for time dispersion calculation.

$$dT = - \frac{D}{V^2} dv - \frac{R}{V} \tan \theta d\theta$$

$$\approx - \frac{R}{V^2} dv - \frac{R}{V} \theta d\theta$$

where

$$R = 50 \text{ miles} = 80,500 \text{ meters}$$

$$V = 1500 \text{ m/sec.}$$

$$dV = 4 \text{ m/sec.}$$

$$\theta = .104 \text{ radians}$$

$$d\theta = .0174 \text{ radians}$$

Carrying out the calculation the time variation is 0.240 sec.

This is a variation from the straight line path, however.

Even the shortest paths will range from the straight line by

.04 - .06 sec. This leaves a total variation of about 0.2

seconds which compares favorably with the only experimental

data available (23).

APPENDIX D

1. Diversity Error Calculation. In part II it is noted that the diversity receiver makes a decision that m_0 is sent if:

$$\sum_{l=1}^{2L} w_{l0} a_{l0}^2 > \sum_{l=1}^{2L} w_{l1} a_{l1}^2$$

where the a_{li} are statistically independent zero mean Gaussian random variables. Since the w_{li} are all approximately equal they will be neglected and the error probability will be computed for making the decision on:

$$\sum_{j=1}^{2L} a_j^2 > \sum_{i=1}^{2L} a_i^2$$

By pairwise addition of the quadrature components on each channel, the decision can also be represented as:

$$\sum_{j=1}^L b_j^2 > \sum_{i=1}^L b_i^2$$

where the b_j and the b_i are statistically independent Rayleigh distributed random variables, with the following probability distributions.

$$p(b_j) = \frac{4b_j}{E_j + N_j} \exp - \frac{2b_j^2}{E_j + N_j} \quad 0 \leq b_j < \infty$$

$$p(b_i) = \frac{4b_i}{N_i} \exp - \frac{2b_i^2}{N_i} \quad 0 \leq b_i < \infty$$

The error probability can be easily calculated if the probabilities of the two sums are known. These will now be put in a closed form. Define a new variable:

$$k_j = b_j^2$$

then it is easily shown that:

$$p(k_j) = \frac{2}{E_j + N_j} \exp - \frac{2k_j}{E_j + N_j}$$

The probability distribution of the sum of the k_j can be found by noting that the characteristic function of the sum of independent random variables is the product of their individual characteristic functions. The characteristic function of k is:

$$\int_0^{\infty} p(k_j) e^{-sk_j} dk_j = \frac{2}{E_j + N_j} \left(\frac{1}{s + 2/E_j + N_j} \right)$$

Therefore the characteristic function of the sum of the k_j is:

$$\int_0^{\infty} p(\sum_{j=1}^L k_j = R_j) e^{-sR_j} dR_j = \prod_{j=1}^L \left(\frac{2}{E_j + N_j} \right) \left(\frac{1}{s + 2/E_j + N_j} \right)$$

By a partial fraction expansion it is easily shown that the probability density function of the sum of the k_j is the sum of L exponentials.

Knowing the probability functions, the probability of error can easily be calculated. If m_0 is sent, and

$$\sum_{d=1}^L k_{d0} = R_0$$

$$\sum_{d=1}^L k_{d1} = R_1$$

then the error probability is:

$$p(\mathcal{E}) = \int_0^{\infty} p(R_1) \int_0^{R_1} p(R_0) dR_0 dR_1$$

This integral can be solved in general. For the special case of two-fold diversity it takes the following form:

$$p(\mathcal{E}) = 1 - \left(\frac{K_3 K_4}{K_3 - K_4} \right) \left[\left(\frac{K_1}{K_1 - K_2} \right) \left(\frac{1}{K_2 + K_4} - \frac{1}{K_2 + K_3} \right) + \left(\frac{K_2}{K_1 - K_2} \right) \left(\frac{1}{K_1 + K_3} - \frac{1}{K_1 + K_4} \right) \right]$$

where:

$$K_1 = \frac{2}{E_1 + N_1}$$

$$K_2 = \frac{2}{E_2 + N_2}$$

$$K_3 = \frac{2}{N_1}$$

$$K_4 = \frac{2}{N_2}$$

This last result is restricted to cases where $K_1 \neq K_2$ and $K_3 \neq K_4$. If one or both of these pairs were equal, the result would be found in a similar way, but would be slightly different. Figure 21 shows the effect of varying signal-noise ratio on two-fold diversity.

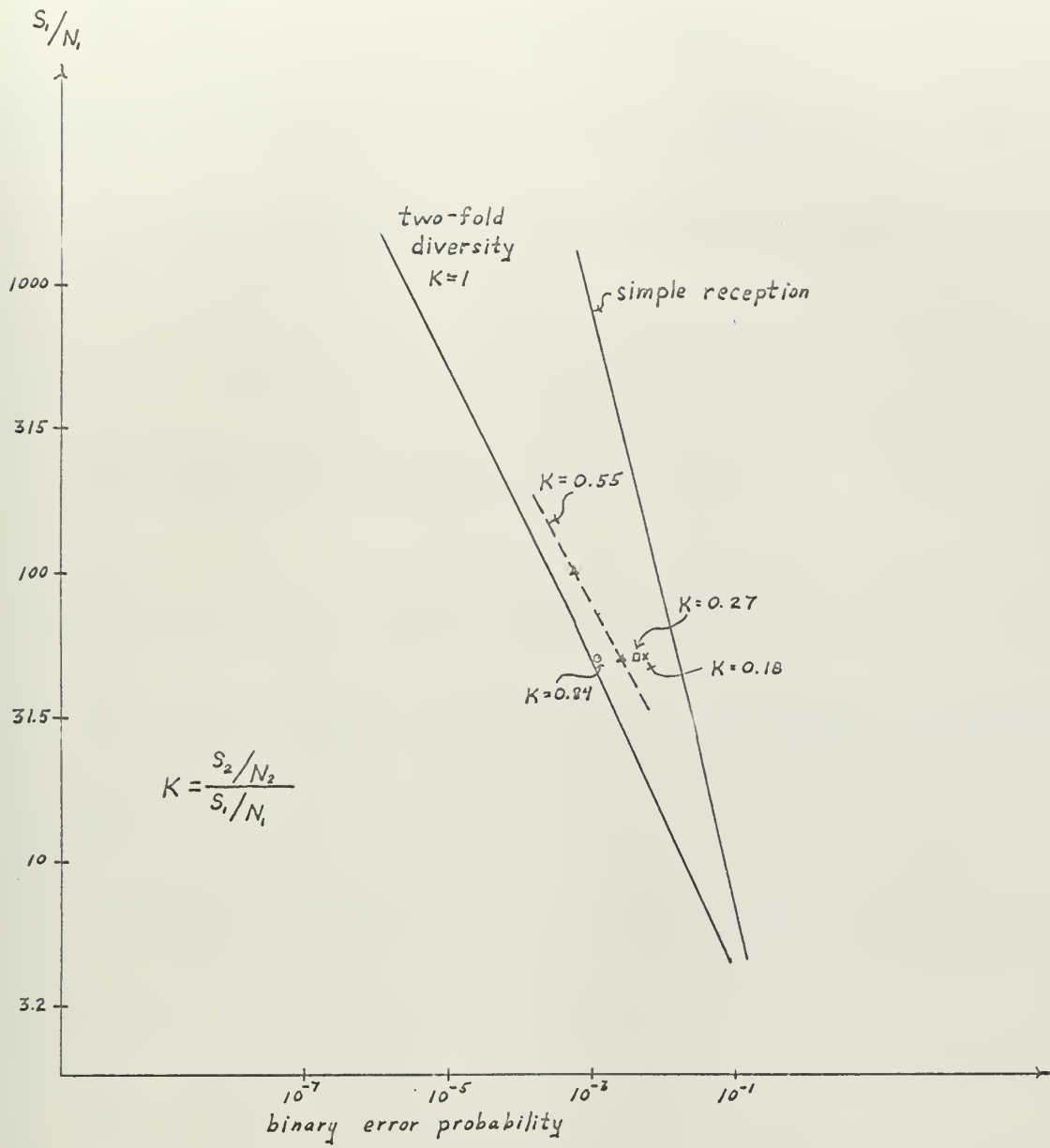


Figure 21. Diversity error with unequal signal-noise ratios.

REFERENCES CITED

1. L.E. Kinsler and A.R. Frey, Fundamentals of Acoustics, Second Ed., (New York, 1962), p. 461.
2. A.C. Kibblewhite and R.N. Denham, "Experiment on Propagation in Surface Sound Channels," JASA,* 38:1, Jan. 1965, pp. 63-66.
3. H.W. Marsh, M. Schulkin, and S.G. Kneale, "Scattering of Underwater Sound by the Sea Surface," JASA, 33:3, March 1961, p. 340.
4. M. Schulkin and H.W. Marsh, "Sound Absorption in Sea Water," JASA, 34:6, June 1962, pp. 864-5.
5. "Physics of Sound in the Sea, Part I: Transmission," NDRC Summary Technical Reports, Division 6, volume 8, pp. 41-49.
6. Ibid. p. 67.
7. K.V. MacKenzie, "Reflection of Sound from Coastal Bottoms," JASA, 32:2, Feb. 1960, pp. 221-231.
8. Carl Eckart, ed., "Principles and Applications of Underwater Sound," NDRC Summary Technical Reports, Division 6, Volume 7, p. 53.
9. Ibid. p. 47.
10. J.D. MacPherson and N.O. Fothergill, "Study of Low-Frequency Sound Propagation in the Hartlen Point Region of the Scotian Shelf", JASA, 34:7, July 1962, pp. 967-971.
11. Kibblewhite and Denham, op. cit., p. 66.
12. K.V. MacKenzie, "Long Range Shallow-Water Transmission," JASA, 33:11, Nov. 1961, pp. 1512-1514.
13. G.M. Wenz, "Acoustic Ambient Noise in the Ocean: Spectra and Sources," JASA, 34:12, Dec. 1965, pp. 1936-1956.
14. Eckart, op.cit., pp. 230-237.
15. Wenz, op. cit., p. 1938.
16. C.L. Piggott, "Ambient Sea Noise at Low Frequencies in Shallow Water of the Scotian Shelf", JASA, 36:11, Nov. 1964, p. 2154.

* Journal of the Acoustical Society of America.

17. C.B. Officer, Introduction to the Theory of Sound Transmission with Application to the Ocean, (New York, 1958), p. 6.
18. J.M. Wozencraft and I.M. Jacobs, Principles of Communication Engineering, (New York, 1965), pp. 527-532.
19. "Physics of Sound in the Sea," pp. 158-164.
20. K.V. MacKenzie, "Long-Range Shallow Water Signal Level Fluctuations and Frequency Spreading," JASA, 34:1, Jan. 1962, p. 70.
21. Ibid. pp. 72-74.
22. H.W. Marsh and R.H. Mellen, "Underwater Sound Propagation in the Arctic Ocean," JASA, 35:4, April 1963, p. 556.
23. J.C. Steinberg and T.G. Birdsall, "Underwater Sound Propagation in the Straits of Florida," JASA 39:2, Feb. 1966, pp. 312-314.
24. H.P. Bucker and H.E. Morris, "Normal-Mode Intensity Calculations for a Constant-Depth, Shallow Water Channel." JASA, 38:6, Dec. 1965, pp. 1010-1017.
25. "Physics of Sound in the Sea," pp. 165-166.
26. G.L. Turin, "Error Probabilities for Binary Symmetric Ideal Reception through Non-Selective Slow Fading and Noise", Proceedings of the I.R.E., 46:9, Sept. 1958, pp. 1603-1619.
27. T. Kailath, "Optimum Receivers for Randomly Varying Channels," Proc. 4th London Symp. Inform. Theory, C. Cherry (Ed.) (Washington, 1961), pp. 109-122.
28. R. Price, "Optimum Detection of Random Signals in Noise, with Application to Scatter-Multipath Communication," I.R.E. Transactions on Information Theory, IT-2:4, Dec. 1956, pp. 125-135.
29. Wozencraft and Jacobs, op. cit. pp. 519-524, 535.
30. C.E. Shannon and W. Weaver, The Mathematical Theory of Communication, (Urbana, Illinois, 1963), p. 39.
31. Ibid. p. 38.
32. R.G. Gallager, "A Simple Derivation of the Coding Theorem and Some Applications," IEEE Trans. on Information Theory, IT-11:1, January 1965, pp. 3-18.

33. Wozencraft and Jacobs, op. cit., p. 538.
34. Ibid. pp. 542-545.
35. W.W. Peterson, Error Correcting Codes, (New York, 1961) p. 71.
36. R.G. Gallager, Low Density Parity Check Coding, (Cambridge, Mass, 1963), p. 7.
37. F.I. Bloom, S.S.L. Chang, B. Harris, A. Hamptschein, K.C. Morgan, "Improvement of Binary Transmission by Null-Zone Reception". I.R.E. Proceedings, 45:7, July 1945, pp. 963-975.
38. P. Elias, "Coding and Decoding", Lectures on Communication System Theory, E.J. Baghdady (Ed.), (New York, 1961), pp. 321-343.
39. Gallager, loc.cit.
40. Wozencraft and Jacobs, op. cit., p. 410.
41. Ibid., pp. 425-439.
42. I.L. Massey, Threshold Decoding, (Cambridge, Mass., 1963), pp. 1-63.
43. Ibid., p. 71.

thesR135

Shallow water hydroacoustic communicatio



3 2768 001 01315 4

DUDLEY KNOX LIBRARY